LIPID NANOPARTICLE DELIVERY OF SMALL INTERFERING RNA TARGETING ANDROGEN RECEPTOR VARIANTS FOR PROSTATE CANCER

by

Joslyn Quick

B.Sc., The University of British Columbia, 2013

A THESIS SUBMITTED IN PARTIAL FULFILLMENT OF

THE REQUIREMENTS FOR THE DEGREE OF

MASTER OF SCIENCE

in

THE FACULTY OF GRADUATE AND POSTDOCTORAL STUDIES

(Biochemistry and Molecular Biology)

THE UNIVERSITY OF BRITISH COLUMBIA

(Vancouver)

April 2019

The following individuals certify that they have read, and recommend to the Faculty of Graduate and Postdoctoral Studies for acceptance, a thesis/dissertation entitled:

LIPID NANOPARTICLE DELIVERY OF SMALL INTERFERING RNA TARGETING ANDROGEN RECEPTOR VARIANTS FOR PROSTATE CANCER

---

submitted by Joslyn Quick in partial fulfillment of the requirements for

the degree of Master of Science

in Biochemistry and Molecular Biology

Examining Committee:

Michel Roberge
Supervisor

Sheila Teves
Supervisory Committee Member

Leonard Foster
Supervisory Committee Member

Scott Covey
Additional Examiner

Additional Supervisory Committee Members:

Supervisory Committee Member

Supervisory Committee Member

Abstract

Expression of constitutively active splice variants of the androgen receptor (AR) currently poses treatment challenges for advanced stages of prostate cancer. Conventional hormone therapies for prostate cancer target the AR ligand-binding domain, which is completely absent in most AR splice variants. Utilizing small interfering RNA (siRNA) as a genetic drug can provide an approach to target such cancer-promoting variants, but requires a vehicle to prevent premature degradation and promote delivery to the cytosol of diseased cells. This thesis investigates the efficacy of a lipid nanoparticle (LNP) carrier of siRNA that specifically targets all AR variant forms (siARv). Two human prostate cancer models were utilized throughout the studies described here: the 22Rv1 cell line exhibits high expression levels of AR splice variants and growth dependency on the like; LNCaP cell growth is dependent on full-length AR and expresses extremely low levels of splice variant forms. A screen in 22Rv1 cells identified siARv from a panel of siRNAs designed against exon 1 of AR mRNA, a target that enables knockdown of full-length and variant ARs. The ability of a clinical-grade LNP formulation containing siARv to facilitate silencing of ARs was demonstrated in 22Rv1 and LNCaP cells, and it was shown that this knockdown of ARs also affected AR transcriptional activity, as exhibited by reduction of prostate-specific antigen levels in both models upon treatment. It was demonstrated that treatment with siARv-LNP reduced the viability of 22Rv1 cells more effectively than LNP carrying siARfl (siRNA targeting full-length AR mRNA only), whereas the effect on LNCaP cell viability of siARv-LNP and siARfl-LNP was not differentiable. The biodistribution of siARv-LNP formulated for optimal *in vivo* activity was measured in mice bearing 22Rv1 xenografts, demonstrating a measurable accumulation of LNP at distal tumors. The antitumor activity of the

siARv-LNP system was subsequently tested on 22Rv1 xenografts upon repeat dosing, exhibiting slowed tumor progression, as well as enhanced survival, compared to animals treated with siARfl-LNP. These results provide an alternative means to target AR variants by way of LNP-mediated gene therapy, and comment on the relative utility of this approach in treating an AR variant-dependent prostate cancer model.

Lay Summary

Prostate cancer cell growth and survival is largely dependent on the androgen receptor (AR). Advanced stages of prostate cancer can express increased levels of variant ARs, which confer resistance to treatments currently available in the clinic. A means to target such AR variants is by use of small interfering RNA (siRNA), a molecule that can be designed to lower specific gene expression levels. However, systemically administered siRNA is prone to degradation and requires a vehicle to promote delivery to diseased cells; use of a clinical-grade carrier, a lipid nanoparticle (LNP) system, can make siRNA a more viable therapeutic approach. In this thesis, the optimization of an AR variant-targeted siRNA, the efficiency of this siRNA once encapsulated in LNP, and the effects of the siRNA-LNP system on human prostate cancer cell health are described. The anticancer effects of the AR variant-targeted siRNA-LNP are also shown in mice bearing human prostate cancer-derived tumors.

Preface

This thesis contains the original unpublished work of the author, Joslyn Quick. I performed all of the experiments and data analysis contained within, with the following exceptions: the cryogenic transmission electron microscopy and imaging shown in Figure 3.5 was performed by Jayesh Kulkarni of the Cullis laboratory; the animal care for experiments shown in Figure 3.10, Figure 3.11, and Figure 3.12 was performed by Nicole Wretham, Nancy Dos Santos, Binab Karmacharya, Maryam Osooly, and Hong Yan of the Investigational Drug Program at the BC Cancer Agency; the tissue digestion for the study shown in Figure 3.10 was performed with the assistance of Roy van der Meel of the Cullis laboratory. The animal research contained within this thesis was performed with ethical approval by the Institutional Animal Care Committee (IACC) at UBC, under protocol #A14-0290.

Table of Contents

List of Tables

List of Figures

List of Abbreviations

2'-O-Me	2'-O-methyl
ANOVA	analysis of variance
ApoE	apolipoprotein E
AR	androgen receptor
AR-V7	androgen receptor spice variant 7
ASO	antisense oligonucleotide
CE3	cryptic exon 3 of androgen receptor mRNA
cryo-TEM	cryogenic transmission electron microscopy
cDNA	complementary DNA
CLU	clusterin
C_T	cycle threshold
DBD	DNA-binding domain
DLin-DMA	1,2-dilinoleyloxy-3-dimethylaminopropane
DLin-KC2-DMA	2,2-dilinoleyl-4-(2-dimethylaminoethyl)-[1,3]-dioxolane
DLin-MC3-DMA	dilinoleylmethyl-4-dimethylaminobutyrate
DNA	deoxyribonucleic acid
DODAP	1,2-dioleoyl-3-dimethyammonium-propane
DSPC	1,2-distearoyl-sn-glycero-3-phosphocholine
ED_{50}	effective dose to achieve 50% gene silencing
EDTA	ethylenediaminetetraacetic acid
EPR	enhanced permeability and retention

FAM	fluorescein amidite
FBS	fetal bovine serum
HRP	horseradish peroxidase
IBFQ	Iowa Black fluorescence quencher
IDT	Integrated DNA Technologies
LBD	ligand-binding domain
LNP	lipid nanoparticle
mRNA	messenger RNA
MTT	3-(4,5-dimethyl-2-thiazolyl)-2,5-diphenyl-2H-tetrazolium bromide
NRG	NOD-*Rag1*^{null} *IL2rg*^{null}
NTD	N-terminal domain
PAGE	polyacrylamide gel electrophoresis
PBS	phosphate buffered saline
PBS-T	phosphate buffered saline with 0.1% Tween-20
PDI	polydispersity index
PEG	polyethylene glycol
PEG-DMG	1,2-dimyristoyl-sn-glycerol-3-methoxypolyethylene glycol
PEG-DSG	1,2-distearoyl-sn-glycerol-3-methoxypolyethylene glycol
PSA	prostate-specific antigen
PSMA	prostate-specific membrane antigen
qPCR	quantitative polymerase chain reaction
RIPA	radioimmunoprecipitation assay
RISC	RNA-induced gene silencing complex

RNA	ribonucleic acid
RNAi	RNA interference
RPMI	Roswell Park Memorial Institute medium
SDS	sodium dodecyl sulfate
siARv	siRNA targeting exon 1 of AR mRNA
siARfl	siRNA targeting exon 8 of AR mRNA
siLUC	siRNA targeting the luciferase gene
siRNA	small interfering RNA
siRNA-LNP	siRNA-lipid nanoparticle

.

Chapter 1: Introduction

1.1 Prostate cancer

Among North American men, prostate cancer is one of the most commonly diagnosed cancers and remains a leading cause of cancer-related death (Siegel et al., 2019). The histological pattern of prostatic tissue samples, serum levels of prostate-specific antigen (PSA), and the location and size of tumors all serve to inform prostate cancer prognoses and treatment plans (D'Amico et al., 1998; Mottet et al., 2017). For patients with early stage disease, defined by serum PSA levels within the range of 4-10 ng/ml and tumors detected upon biopsy, active surveillance of disease progression is a preferred alternative to immediate intervention (Lawrentschuk & Klotz, 2011). Prostatectomy and radiation were early developments in the treatment of prostate cancer (Bagshaw et al., 1965; Walsh et al., 1983), and are routine procedures for patients with rising serum PSA levels and tumors that remain localized to the prostate but are large enough to be felt by digital rectal exam (Litwin & Tan, 2017). In 1941, the pioneering efforts of Huggins and Hodges demonstrated the benefit of surgical castration in men with advanced metastatic prostate cancer, a strategy after which clinical practice continues to be modeled (Huggins & Hodges, 1941). Chemical castration, or androgen deprivation therapy (ADT), is now the front-line treatment for men who present with advanced stages of prostate cancer or men with a recurrence following definitive treatment, and operates through the function of the androgen receptor (AR), a key player in the promotion of prostate cancer growth and survival.

1.1.1 The androgen receptor

The AR is an androgen-dependent nuclear transcription factor. The AR gene is located on the X chromosome and encodes eight exons, which are transcribed into the 919 amino acids of the AR protein. The structure of the AR protein consists of an N-terminal domain (NTD), a DNA-binding domain (DBD), a hinge domain (HD), and a ligand-binding domain (LBD) (Lonergan & Tindall, 2011). The NTD contains a transcriptional activation function, AF-1, which is essential for the transcriptional activity of the AR (Callewaert et al., 2006). The NTD has therefore been described as the 'Achilles heel' of the AR, as no transcriptional activity of AR exists in NTD deletion mutants (Sadar, 2011). This domain also exhibits a high degree of intrinsic disorder, making it a difficult target for structure-based drug design (McEwan, 2012). The DBD consists of two zinc fingers that recognize DNA consensus sequences and facilitate direct DNA binding of the AR to the promoter and enhancer regions of AR-regulated genes (Lonergan & Tindall, 2011). Another transcriptional activation function, AF-2, is located in the LBD and is important for mediating direct interactions between the NTD and LBD of the AR to stabilize bound androgens and for binding of coregulators (He et al., 1999). The AR is localized to the cytoplasm in the absence of androgen activation, associated with heat-shock and other chaperone proteins via the LBD (Fang et al., 1996). Testosterone and its more biologically active derivative, dihydrotesterone (DHT), are androgenic hormones that mediate their actions via the AR LBD. The AR binds with strong affinity in the low nanomolar range with DHT, a 2-fold higher affinity compared to that of testosterone (Grino et al., 1990). When the AR LBD binds androgen, a conformational change occurs that results in the dissociation of chaperone proteins, interaction of the NTD and LBD, and translocation to the nucleus. In the nucleus, the AR forms homodimers and interacts with androgen response elements in the promoter regions of

AR-regulated genes (van Royen et al., 2012). For example, the promoter of the PSA gene includes several binding sites for the AR and activation of the AR leads to transcription and translation of PSA (Cleutjens et al., 1996).

1.1.2 Androgen deprivation therapy

For advanced prostate cancer, disease that has spread beyond the prostate to lymph nodes, bone, or other organs, ADT is the mainstay of treatment. Conventional ADT by surgical castration has largely been superseded by luteinizing hormone-releasing hormone (LHRH) therapy, which serves to chemically reduce bodily testosterone production (Sathianathen et al., 2018). Binding of LHRH to its receptor in the anterior pituitary gland triggers the release of luteinizing hormone, which stimulates the testes to synthesize testosterone. LHRH agonists stimulate the receptor, generating a transient surge in testosterone that is followed by down-regulation of the receptor and subsequent suppression of testosterone production (Cooke & Sullivan, 1985; Ahmann et al., 1987). Conversely, LHRH antagonists competitively bind to and block LHRH receptors, inhibiting leuteinizing hormone release and promoting testosterone suppression (Crawford & Hou, 2009). Conventional ADT has also been achieved through the use of first generation anti-androgen drugs, such as bicalutamide, flutamide, and nilutamide, all non-steroidal molecules that directly bind the AR LBD and compete with androgen signaling (Soloway et al., 1995; Yoshimura et al., 2003; Nakabayashi et al., 2005). Anti-androgens can be used in combination with LHRH agonists to mitigate the testosterone surge, or dosed in combination with an LHRH antagonist, to achieve what is referred to as complete androgen blockade (Labrie et al., 1983; Cornford et al., 2017). Although this approach remains effective

in improving both survival and symptoms, ADT is not curative and castration-resistant disease inevitably develops.

1.2 Castration-resistant prostate cancer

The AR pathway continues to play a major role in castration-resistant prostate cancer, disease that progresses with elevated serum PSA levels or the appearance of metastases despite castrate levels of androgen signaling. The molecular mechanisms underlying the reactivation of AR signaling include amplification of the AR gene, coactivator gain of function or loss of corepressor function, and intratumoral androgen synthesis (Sharp et al., 2016). The first AR LBD point mutation, T878A, was identified in the LNCaP prostate cancer cell line (Veldscholte et al., 1990), and was later detected in a clinical specimen of castration-resistant prostate cancer (Suzuki et al., 1993). Since this discovery, the AR LBD has emerged as a mutational hotspot, with T878A, W742C, H875Y, and L702H characterized as recurrent AR LBD point mutations and showing up in ~20% of castration-resistant cases (Beltran et al., 2013). These mutations alter the ligand-binding affinity of the AR and cause signal hypersensitivity. They can cause binding flexibility in the LBD, allowing the AR to become activated by adrenal steroids, progesterone, glucocorticoids, estrogens, and anti-androgens (Eisermann et al., 2013). Considerable focus has more recently been placed on AR splice variants as a mechanism for castration resistance.

AR splice variants arise from alternatively spliced AR mRNA, the protein products of which contain the NTD and the DBD, but are truncated at the C-terminus and lack the LBD. All licensed therapies that modulate AR signaling do so through the function of the AR LBD, and have little or no activity against such AR variants. These AR splice variants are constitutively

active, and can activate the full-length AR in the absence of androgen to facilitate transcription of androgen-controlled genes (those involved in biosynthesis and metabolism), as well as mediate the expression of a distinct gene signature that is independent of androgens (cell cycle genes) (Hu et al., 2012; Cao et al., 2014). Over 20 AR splice variants have been discovered in castration-resistant specimens, with 8 of those detected at comparably low rates in benign tissue (Robinson et al., 2015); however, AR-V7 is the most frequently observed and the most abundantly expressed AR variant in the clinic. It has also been shown that AR-V7 is the most highly expressed variant in several prostate cancer cells lines, including 22Rv1 and LNCaP cells, again suggesting that AR-V7 is the primary AR splice variant (Guo et al., 2009). AR-V7 mRNA is composed of exons 1-3 and cryptic exon 3 (CE3), which encodes 16 variant-specific amino acids at the C-terminus. There is evidence that AR-V7 mRNA is detectable in normal prostatic tissues, in about 6% of patient samples (Ware et al., 2014), and that AR-V7 levels increase as patients progress from hormone-sensitive to castration-resistant prostate cancer (Ware et al., 2014; Welti et al., 2016). Moreover, AR-V7 detected in primary prostate cancer tissues is associated with castration resistance and shorter survival (Hornberg et al., 2011). Due to the persistent signaling of AR variants in the castration-resistant setting, there is continued interest in the development of therapeutic agents that specifically target this adaptive AR aberration.

1.2.1 Treatment of castration-resistant prostate cancer

This late-stage disease is currently incurable, and the aim of treatment for castration-resistant prostate cancer is to increase overall survival and promote quality of life for the patient (Cornford et al., 2017). Docetaxel, a taxane chemotherapeutic that works by disrupting microtubules and thereby stopping cell division, was the first treatment to show an improvement

in overall survival of patients (Tannock et al., 2004; Berthold et al., 2008). Cabazitaxel has since been utilized to overcome the emergence of taxane resistance, showing antitumor activity in post-docetaxel patients (de Bono et al., 2010). Sipuleucel-T is the only immunotherapy approved for the treatment of castration-resistant prostate cancer (Kantoff et al., 2010; Wei et al., 2015); however, this drug is not widely used due to adverse side effects and the exorbitant cost (Simpson et al., 2015). Two compounds that specifically target the AR signaling pathway have been of great clinical importance in the castration-resistant setting. Firstly, abiraterone acetate functions to block androgen production by inhibiting the cytochrome p450 17A1 (CYP17A1) enzyme. CYP17A1 is required for the production of androgenic hormones in the adrenal glands, testes, and prostatic tumors (Attard et al., 2005). Secondly, enzalutamide is an anti-androgen that offers a treatment advantage over first-generation anti-androgens. Enzalutamide not only antagonizes full-length AR, but also prevents AR nuclear translocation, AR binding to DNA, and coactivator recruitment by AR (Tran et al., 2009; Scher et al., 2012). The AR splice variant AR-V7 has been associated with resistance to both abiraterone acetate and enzalutamide, as AR-V7 expression levels increase after castration-resistant disease progresses on each treatment (Antonarakis et al., 2014).

1.2.2 Strategies for targeting androgen receptor variants

As the role for AR variants in the development and progression of castration-resistant prostate cancer has become more apparent, several strategies have been investigated for targeting AR variant activity (Antonarakis et al., 2016). One approach aimed at reducing the function of variant ARs includes targeting their synthesis, either by inhibiting AR splicing (Ferraldeschi et al., 2016) or by blocking AR CE3 polyadenylation (Van Etten et al., 2017). Preventing the

initiation of transcription by AR has also been explored. Use of bromodomain-containing protein 4 (BRD4) inhibitors blocks this coregulator's interaction with AR, and prevents binding of both full-length and splice variant AR to chromatin (Asangani et al., 2014; Chan et al., 2015). An approach that has advanced to clinical development involves the direct degradation of the AR variant protein. Niclosamide was identified through chemical screening efforts to induce AR-V7 protein degradation (C. Liu et al., 2014), and has shown significant anti-tumor activity in a number of AR variant expressing cell lines, including 22Rv1 cells, as well as in 22Rv1 xenografts with abiraterone acetate and enzalutamide resistance (C. Liu et al., 2016). A current clinical trial (NCT02807805) investigating niclosamide in combination with abiraterone acetate in patients with castration-resistant prostate cancer has shown improved efficacy of the combination treatment over abiraterone acetate alone (Pan et al., 2018). Direct inhibitors of the AR NTD represent another strategy to treating prostate cancer. EPI-506 directly binds the NTD of AR and its variants, inhibiting transcriptional activity (Andersen et al., 2010; Myung et al., 2013; Yang et al., 2016). A clinical trial (NCT02606123) investigating the use of EPI-506 in men with castration-resistant prostate cancer that had progressed on enzalutamide or abiraterone acetate showed long-term stable disease at the higher dose levels in some patients, indicating signs of utility of AR NTD targeting in the clinic. However, the study was terminated early due to high pill burden, suggesting the need for a more potent derivative. Although met with challenges, the AR NTD remains an attractive therapeutic target for the development of drugs to treat castration-resistant forms of prostate cancer. The approach that is proposed in this thesis is to hijack the RNA interference machinery and target the region of AR mRNA that encodes the NTD.

1.3 RNA interference and gene silencing

RNA interference (RNAi) was first described in 1998, with the discovery that double-stranded RNA could silence gene expression in *Caenorhabditis elegans* (Fire et al., 1998). Sequence-specific gene knockdown with exogenous small interfering RNA (siRNA) was subsequently demonstrated in mammalian cells (Elbashir et al., 2001), followed by the first successful use of synthetic siRNA for gene silencing in mice (McCaffrey et al., 2002). Synthetic siRNA duplexes are typically composed of 19-22 nucleotides, a length that is sufficient to be recognized by RNAi machinery but short enough to avoid the immune response provoked by duplexes greater than 30 nucleotides in length (Gantier & Williams, 2007). These siRNAs mimic the product of Dicer cleavage, and interact directly with the RNA-induced silencing complex (RISC) in the cytoplasm of cells. The endonuclease argonaute 2 (AGO2) component of RISC then separates the passenger strand (sense strand) of the siRNA from the guide strand (antisense strand), which remains associated with the RISC and directs it to the target mRNA (Pecot et al., 2011). The complementary binding of the guide strand with the target mRNA activates the AGO2, which then cleaves the mRNA between bases 10 and 11 relative to the 5′ end of the guide strand. Exonucleases present in the cell perform complete degradation of the mRNA after the initial cleavage made by AGO2. The activated RISC complex, loaded with the guide strand, can then move on to destroy additional mRNA targets, which further propagates gene silencing (Valencia-Sanchez et al., 2006). Increasing the length of the siRNA duplexes to 25-27 nucleotides has been shown to enhance potency over conventional siRNAs (Kim et al., 2004; Rose et al., 2005). These longer siRNAs require processing by Dicer into the shorter siRNAs, and are termed Dicer-substrate siRNAs. It has been proposed that these Dicer

substrates are more efficiently loaded into the RISC, thus facilitating an enhanced and prolonged gene-silencing effect (Hefner et al., 2008).

The degradation half-life reported for free, unmodified siRNA in human plasma is on the order of minutes, thus a wide range of chemical modifications have been investigated to enhance siRNA stability against degradation by nucleases, without jeopardizing gene-silencing activity. The replacement of the non-bridging oxygen of the phosphate backbone with sulfur (phosphorothioate) at the 3' ends can provide protection against nuclease degradation, while minimizing the overall phoshporothioate content which can otherwise reduce potency and/or cause toxicity (Behlke, 2008). The 2' position of the ribose can also be modified to confer resistance to nuclease degradation, with the addition of a methyl group (2'-O-Me) for example. 2'-O-Me modifications are naturally occurring and do not induce significant toxicity, and are well tolerated in most positions of the siRNA (Behlke, 2008). Unmodified synthetic siRNA may also activate an unwanted immune response. Toll-like receptors 3, 7, and 8, which are present in endosomal compartments, may trigger an immune response when synthetic siRNA enters the cell. This immune response can be avoided in the same way siRNA can be designed to evade nuclease degradation, through the incorporation of 2'-O-Me modifications. Inclusion of only two or three 2'-O-Me modified residues can be sufficient to prevent immune activation by synthetic siRNA (Judge et al., 2006).

Although advances in siRNA design offer increased stability and reduced immunogenicity, free siRNA does not efficiently accumulate in many target tissues upon systemic administration, and cannot readily cross cell membranes to reach the cytoplasmic site of action; therefore, an effective delivery vehicle is required to realize the full therapeutic potential (Whitehead et al., 2009). Lipid nanoparticles (LNP) containing ionizable amino lipids are the

leading system for intravenously administered siRNA drugs. Recently, Alnylam Pharmaceuticals' Patisiran, an LNP containing siRNA targeted to transthyretin in the liver, was clinically approved for the treatment of hereditary transthiritin amyloidosis (Adams et al., 2018).

1.4 Development of LNP for siRNA

The first description of liposomes came with the discovery that dispersions of lecithin and cholesterol assemble into concentric lamellae (Bangham & Horne, 1964), and eventually the potential for using liposomes as drug delivery systems was established (Gregoriadis & Ryman, 1971; Gregoriadis, 1973). The transmembrane pH gradient loading technique was a major development in the field, allowing for the liposomal entrapment of weakly basic molecules (Nichols & Deamer, 1976). This technique relies on the deprotonated form of weakly basic compounds at an external neutral pH to readily diffuse across the liposomal membrane, becoming protonated and trapped in an acidic interior. By this method, it was shown that chemotherapeutic drugs like doxorubicin could be efficiently loaded and retained in liposomal systems of phosphatidylcholine and cholesterol (Mayer et al., 1986a). In the context of drug delivery, liposomes serve to protect their cargo from degradation, as well as improve the pharmacokinetic profile and targeting of drugs towards specific tissues upon intravenous administration (Kimelberg et al., 1976; Juliano & Stamp, 1978). The vasculature at disease sites like solid tumors exhibits defective architecture compared to that of healthy tissues. Long-circulating liposomes with a diameter of <100 nm tend to preferentially accumulate at these sites, a phenomenon known as the enhanced permeation and retention (EPR) effect (Maeda, 2001). Several liposomal drugs have been approved for clinical use, with most containing chemotherapeutic drugs that rely on this ability of LNP systems to preferentially extravasate at

tumor sites following intravenous administration (Allen & Cullis, 2013). The design of LNP systems for the delivery of nucleic acids has been modeled after the aforementioned liposomal technology for small-molecule drugs; however, the size and negative charge of nucleic acids requires an alternative loading and entrapment method. The incorporation of cationic lipids in the LNP formulation facilitated the encapsulation of nucleic acids (Felgner et al., 1994), and the later use of ionizable amino lipids overcame issues that arose with permanently charged cationic lipid such as dose-limiting toxic side effects (Lv et al., 2006). Ionizable amino lipid-containing siRNA-LNP systems first showed significant gene knockdown in hepatocytes following intravenous administration (Zimmermann et al., 2006), leading to the extensive optimization of these systems for liver targets.

1.4.1 Lipid composition of siRNA-LNP

The LNP systems currently utilized in the clinic for hepatic gene silencing consist of an ionizable amino lipid (dilinoleylmethyl-4-dimethylaminobutyrate, DLin-MC3-DMA), a phosphatidylcholine lipid (1,2-distearoyl-sn-glycero-3-phosphocholine, DSPC), cholesterol, and a polyethylene glycol (PEG) lipid (1,2-dimyristoyl-sn-glycerol methoxypolyethylene glycol, PEG-DMG) (Adams et al., 2018). The optimized lipid composition consists of DLin-MC3-DMA/DSPC/cholesterol/PEG-DMG at a molar percentage (mol%) of 50/10/38.5/1.5, respectively (Jayaraman et al., 2012). These advanced siRNA delivery vehicles have a relatively short circulation half-life compared to those of long-circulating liposomes, and are produced at diameters <100 nm which allows the LNP to readily pass the liver fenestrae and interact with hepatocytes for target gene silencing (Chen et al., 2016).

The ionizable amino lipid component of the LNP system entraps nucleic acids via charge interactions during the formulation process at acidic pH and maintains a neutral surface charge at physiological pH (Maurer et al., 2001; Semple et al., 2001). This lipid also facilitates endosomal escape of the siRNA payload by destabilizing the anionic endosomal membrane through interactions with the positive charge of the amino moiety (Hafez et al., 2001). The first ionizable amino lipid utilized for the encapsulation of nucleic acids was 1,2-dioleoyl-3-dimethyammonium-propane (DODAP), having one double bond in each of its acyl chains and an apparent pKa just below 7 (Maurer et al., 2001; Semple et al., 2001). An ionizable amino lipid containing lipid chains with two double bonds, 1,2-dilinoleyloxy-3-dimethylaminopropane (DLin-DMA), subsequently showed improved *in vitro* gene silencing over lipids containing fully saturated lipid chains or chains with one cis double bond (Heyes et al., 2005). It was suggested that the increased ability of the unsaturated lipid to form the inverted hexagonal phase with the anionic endosomal membrane lead to destabilization of the membrane, release of the siRNA to the cytosol, and thus an increased gene-silencing potency. Those ionizable amino lipids with lipid chains containing three cis double bonds exhibited reduced siRNA encapsulation efficiency (Heyes et al., 2005), and subsequent structure optimization was based around DLin-DMA derivatives. Several linker chemistries between the lipid amino head group and lipid chains were evaluated for *in vivo* hepatic gene-silencing activity, demonstrating that the incorporation of a ketal-based linker, 2,2-dilinoleyl-4-(2-dimethylaminoethyl)-[1,3]-dioxolane (DLin-KC2-DMA), conferred a 100-fold increase in LNP potency compared to DLin-DMA (Semple et al., 2010). The apparent pKa of the ionizable amino lipid formulated in the LNP systems was then shown to be a critical structural parameter, and the most potent formulation to date is based on DLin-MC3-

DMA, having an apparent pKa of 6.4 and an ED_{50} (effective dose to achieve 50% hepatic gene silencing) of 0.005 mg per kg bodyweight (Jayaraman et al., 2012).

The presence of PEG lipid in the siRNA-LNP formulation prevents aggregation during LNP production or in circulation upon systemic administration, and serves to shield the LNP surface from opsonins and clearance by the mononuclear phagocyte system (Allen, 1994; Belliveau et al., 2012). However, it has been shown that apolipoprotein (ApoE) adsorbs to LNP and mediates hepatocyte uptake via the low-density lipoprotein receptor. When siRNA-LNPs were administered to ApoE knockout mice, gene-silencing potency was reduced and could be rescued by preincubation of LNP with ApoE (Akinc et al., 2010). Although PEG lipid is essential for LNP stability, the potential for it to decrease interactions with ApoE and interfere with transfection of hepatocytes is a parameter that must be considered in the design of these systems. Moreover, PEG lipids can reduce the interaction and fusion required for the endosomal release of siRNA into the cytoplasm (Gilleron et al., 2013). In order to maximize hepatic gene silencing *in vivo*, the density of PEG lipid is reduced to the minimum to support self-assembly and stability (1.5 mol%), and the acyl chains of PEG lipid are kept relatively short (PEG-DMG with dimyristoyl chains) to promote shedding of this LNP-coating lipid following intravenous administration (Mui et al., 2013). By altering the PEG lipid anchor length and density, LNP pharmacokinetics and tissue distribution may be tuned for extrahepatic applications, such as distal tumor sites. The use of PEG lipid with distearyl chains (PEG-DSG) and an increased density of PEG lipid in the siRNA-LNP formulation are both approaches that have been taken to increase circulation times and increase accumulation in tumor tissue (Yamamoto et al., 2015a; Lee et al., 2016). These efforts will be discussed further in Section 1.5.

1.4.2 Production and formation of siRNA-LNP

A common production method for liposomal systems involves the hydration of a lipid film with aqueous buffer, followed by a size reduction method such as extrusion. In the extrusion process, particles in suspension are forced through a polycarbonate filter to form unilamellar vesicles with sizes dictated by the filter pore size (Mayer et al., 1986b). Based on this conventional method for the production of liposomes, the preformed vesicle method was adopted for the formation of nucleic acid-containing systems (Maurer et al., 2001). This approach involves mixing a suspension of extruded vesicles (comprised of ionizable amino lipid, DSPC, cholesterol, and PEG lipid) in 40% ethanol with nucleic acid in low pH buffer. This is followed by dialysis in neutral pH to remove ethanol and neutralize the ionizable amino lipid, and results in multilamellar vesicles that are ~100 nm in size with encapsulation efficiencies of ~80% (Maurer et al., 2001). It was proposed that nucleic acid associates with the surface of the liposome, creates an adhesion point between liposomes that results in the formation of the multilamellar vesicles, and results in nucleic acid that is entrapped between lamellae of the particle. More recently, rapid mixing microfluidic techniques been developed to offer an even more simplified and efficient manner of siRNA-LNP production.

Microfluidic mixing using a staggered herringbone mixer for the production of LNP systems involves the rapid mixing of a lipid-containing ethanol stream with a nucleic acid-containing aqueous stream in a grooved microchannel. It is thought that the increase in polarity of the lipid environment results in the self-assembly and formation of LNP systems, and that LNP adopt the smallest thermodynamically stable size based on the physical properties of lipids and the overall lipid composition (Zhigaltsev et al., 2012). For siRNA-LNP formulated at flow rates >0.2 ml/min, monodisperse particles of reproducible size are achieved with encapsulation

efficiencies over 95% (Belliveau et al., 2012). The size of the siRNA-LNP system can be tuned by varying the amount of PEG lipid within the particle. Particles containing 0.5 mol% PEG lipid exhibit a size of ~80 nm, and by increasing the PEG lipid density to 5 mol%, particle size can be reduced to ~30 nm (Chen et al., 2016). Using cryogenic transmission electron microscopy (cryo-TEM) it was shown that siRNA-LNP had an electron-dense core, and in silico simulations hypothesized that these systems consist of inverted micelles of ionizable amino lipid complexed with or without siRNA (Leung et al., 2012). It was proposed that the relatively hydrophobic complexes of siRNA and ionizable amino lipid precipitate out of solution first and act as nucleation point for subsequent coating with a layer of polar lipids such as PEG lipid, DSPC, and cholesterol (Belliveau et al., 2012; Leung et al., 2012).

Production of nucleic acid-containing LNP systems can also be achieved by use of a T-junction mixer, whereby two input streams are rapidly mixed in a T-shaped chamber (Hirota et al., 1999; Jeffs et al., 2005; Kulkarni et al., 2017). Under optimized total flow rates (>10 ml/min), this mixing technique can produce monodisperse lipidic systems of controlled size and morphology, which are dictated by the LNP composition (Kulkarni et al., 2017). Recently, cryo-TEM was utilized to illustrate that this T-junction mixing method generates siRNA-LNP with similar size and morphology to those formulated with the staggered herringbone mixer technique (Kulkarni et al., 2018). This study also utilized cryo-TEM evidence to describe an alternative mechanism of formation of siRNA-LNP systems. It was proposed that under the formulating conditions (pH 4), small vesicles first arise that contain siRNA complexed with the positively charged headgroup of ionizable amino lipid. Here, these complexes are sandwiched between apposing lipid monolayers. When the pH is then raised to 7.4 upon dialysis of the LNP systems, the siRNA remains trapped in these structures, while any free, uncomplexed neutralized

ionizable amino lipid is deposited in the core of the LNP. PEG lipid, as well as DSPC and cholesterol in part, make up a surface monolayer (Kulkarni et al., 2018).

1.5 LNP delivery of siRNA for silencing the AR

The feasibility of LNP delivery of siRNA for silencing AR gene expression was first demonstrated in the LNCaP model of human prostate cancer (Lee et al., 2012). Here, *in vitro* screening studies compared the potency of a panel of ionizable amino lipids that were originally designed to mediate hepatic gene silencing, and demonstrated that AR siRNA-LNPs containing DLin-KC2-DMA lipid exhibited the most potent silencing effects in LNCaP cells. This was attributed to an optimized ability of DLin-KC2-DMA-LNP to be taken up into cells and to subsequently release the siRNA into the cell cytoplasm (Lee et al., 2012). These results were in agreement with the *in vivo* hepatocyte gene silencing trends (Semple et al., 2010), and demonstrated a similar sensitivity to changes in the structure of the ionizable amino lipid that is incorporated into the LNP. Mice bearing LNCaP xenografts and treated with repeat daily doses of DLin-KC2-DMA-LNP containing AR siRNA maintained baseline levels of serum PSA, as well as significantly reduced xenograft levels of AR protein (Lee et al., 2012). This was the first demonstration that LNP containing ionizable amino lipids, originally optimized for gene knockdown in the liver, could be adapted for knockdown of AR levels at distal tumor sites. These results also implied that the ionizable amino lipid component of the LNP system that facilitates maximum gene-silencing potency in hepatocytes would maintain maximum potency in human prostate cancer-derived cells as well.

1.5.1 Targeted LNP for delivery of siRNA designed against the AR

To improve upon the extrahepatic potency of the siRNA-LNP system, alterations in the PEG lipid content of the LNP formulation, as well as targeting of the prostate cancer cell surface receptor, prostate-specific membrane antigen (PSMA), were investigated (Lee et al., 2016). The previous LNCaP xenograft study utilized PEG lipid with dimyristoyl chains; however, these lipids rapidly exchange out of LNP with half-times on the order of minutes following intravenous injection (Mui et al., 2013). Based off of these findings, the pharmacokinetic properties of LNP containing PEG-DSG were compared, and it was shown that increasing the concentration of PEG-DSG lipid from 2.5 mol% to 5 mol% resulted in a marked increase in circulation half-times from approximately 30 minutes to over 8 hours. Additionally, systems containing 5 mol% PEG-DSG exhibited an approximately fourfold accumulation in distal xenograft tumor tissues compared to those systems with 2.5 mol% PEG-DSG (Lee et al., 2016). A PSMA-targeted moiety (Glu-urea-Lys) was chemically linked to PEG-DSG, and incorporated into an LNP system containing AR siRNA (siARfl) and a total of 5 mole % PEG-DSG to facilitate intracellular uptake into tumor cells following systemic administration. In an LNCaP xenograft model, decreases in serum PSA, tumor cell proliferation, and tumor AR levels were observed following repeat intravenous injections of the PSMA-targeted siARfl-LNP system over two weeks. Non-targeted siARfl-LNP systems were not able to exhibit improved anticancer effects over that of the PBS control group, highlighting the utility of the PSMA-targeting ligand in a system containing a relatively high density of PEG-DSG (Lee et al., 2016). These results suggested that increasing the circulation lifetime and tumor accumulation of LNP by increasing the density of PEG-DSG reduces efficacy of non-targeted systems, and that utilizing a high

molar content of PEG-DSG is not be a viable isolated approach to increasing extrahepatic potency of siRNA-LNP systems.

1.5.2 Combination of siRNA-LNP and AR-targeted antisense oligonucleotide

The efficacy of siRNA tumor delivery using LNP systems has also been tested in an enzalutamide-resistant prostate cancer model, in combination with an AR-targeted antisense oligonucleotide (AR-ASO) (Yamamoto et al., 2015a). Here, LNP were utilized in the delivery of siRNA targeting clusterin, a molecular chaperone induced by AR pathway inhibition to facilitate adaptive survival pathway signaling. Treatment with AR-ASO plus DLin-MC3-DMA-LNP with 2.5% or 5% PEG-DSG containing CLU-siRNA was administered over three weeks. CLU-siRNA-LNP with 2.5% PEG-DSG more effectively enhanced the growth inhibition effects of AR-ASO, silenced the clusterin gene, and reduced serum PSA levels compared to the CLU-siRNA-LNP containing 5 mol% PEG-DSG in mice bearing enzalutamide-resistant LNCaP xenografts (Yamamoto et al., 2015a). These results further highlighted the reduction in potency of LNP systems containing a high molar content of PEG-DSG at extrahepatic tumor sites, despite the increased circulation lifetime that these systems exhibit. This points to the importance of increasing circulation lifetime of LNP carriers to promote tumor accumulation, while at the same time not impeding their interactions with target cells.

Although the accumulation of LNP in the liver has become a major obstacle to extrahepatic delivery, DLin-MC3-DMA-based LNP, as well as systems utilizing earlier-generation ionizable amino lipids, have shown efficacy in various prostate cancer models with repeat dosing, use of a more stably retained PEG lipid, as well as an ‘optimized’ PEG lipid density. These alterations to the canonical, hepatocyte-targeted LNP carrier work to improve the

biodistribution of LNP systems to the tumor site, while maintaining LNP delivery of siRNA to the cytosol of tumor cells.

1.6 Thesis objective

Advanced stages of prostate cancer are currently incurable, with the AR acting as a central driver of the disease, and remaining the main target for therapy in the clinic. Attempts at targeting splice variant forms of the AR for treatment of prostate cancer are prevalent, as these variants are constitutively active and their expression has been linked to the occurrence and progression of castration-resistance. The overall objective of this thesis was to optimize an siRNA molecule for silencing of cancer promoting wild-type and splice variant AR mRNA, utilizing a lipid nanoparticle system to facilitate delivery and transfection of this nucleic acid drug. Lipid nanoparticles are currently the most advanced delivery system for the systemic administration of siRNA, with previous studies demonstrating their utility in the treatment of human prostate cancer models. After optimization of an AR variant-targeted siRNA (siARv), delivery by LNP systems facilitated knockdown of ARs and inhibition of AR transcriptional activity in human prostate cancer cells *in vitro*. As this siARv-LNP system exhibited inhibitory effects on a broad AR population, it also reduced the viability of prostate cancer cells with varying AR molecular phenotypes *in vitro*. The biodistribution of the siARv-LNP systems with an increased lipid-to-siRNA ratio, compared to previous systems tested on human prostate cancer-derived tumors, was also measured in an AR variant-expressing xenograft tumor model, prior to testing the *in vivo* antitumor activity of the siARv-LNP in the same model. Here, the siARv-LNP formulation, upon repeat dosing, exhibited slowed tumor progression and increased survival of treated animals over the PBS control group.

Chapter 2: Materials and Methods

2.1 Materials

1,2-distearoyl-sn-glycero-3-phosphocholine (DSPC) was purchased from Avanti Polar Lipids (Alabaster, AL) and cholesterol was obtained from Sigma-Aldrich (St. Louis, MO). Biofine International (Vancouver, BC) synthesized dilinoleylmethyl-4-dimethylaminobutyrate (DLin-MC3-DMA) as previously described (Jayaraman et al., 2012). 1,2-dimyristoyl-sn-glycerol-3-methoxypolyethylene glycol (PEG-DMG) was provided by Alnylam Pharmaceuticals (Cambridge, MA, USA) or was synthesized as previously described (Akinc et al., 2008). 1,2-distearoyl-sn-glycerol-3-methoxypolyethylene glycol (PEG-DSG) was provided by Alnylam Pharmaceuticals.

2.2 Cell culture

All cell lines used were obtained from the American Type Culture Collection (Manassas, VA) or were a kind gift from Dr. Paul Rennie (Vancouver Prostate Center, Vancouver, BC). 22Rv1 and LNCaP cells were maintained in RPMI-1640 medium supplemented with 10% (v/v) fetal bovine serum (FBS). PC3 cells were grown in Dulbecco's Modified Eagle Medium supplemented with 10% FBS. All cell lines were incubated at 37°C in a 5% CO_2 environment. All cell culture media and reagents were obtained from Gibco (Thermo Fisher Scientific, Valencia, CA). Cells were not passaged beyond 6 months of receipt or resuscitation.

2.3 Quantitative reverse transcription PCR

Total RNA was extracted from cells using an Invitrogen PureLink RNA Mini Kit (Thermo Fisher Scientific) according to the manufacturer's instructions. A NanoDrop™ Lite Spectrophotometer (Thermo Fisher Scientific) was used to determine RNA concentrations. One microgram of total RNA was used as template for cDNA synthesis using a High-Capacity cDNA Reverse Transcription Kit (Applied Biosystems, Foster City, CA). Quantitative PCR (qPCR) was performed using respective cDNA template and TaqMan® Fast Advanced Master Mix (Applied Biosystems) following manufacturer's protocol. Standardized primer-probe assays were purchased from Integrated DNA Technologies (IDT; Coralville, IA). The primer-probe assay for the AR gene was as follows: primer 1, 5'-TCGGACACACTGGCTGTA-3'; primer 2, 5'-TGTCAACTCCAGGATGCTCT-3'; probe, 5'-TCGCCCCTGATCTGGTTTTCAATGA-3'. The primer-probe assay for AR-V7 mRNA consisted of the following: primer 1, 5'-TTGTCCATCTTGTCGTCTTCG-3'; primer 2, 5'-CAATTGCCAACCCGGAATTT-3'; probe, 5'-TGAAGCAGGGATGACTCTGGGAGA-3'. The PSA gene was assayed using the following primer-probe combination: probe, 5'-CCAGGTATTTCAGGTCAGCCACAGC-3'; primer 1, 5'-CGATTCTTCAGGAGGCTCAT-3'; primer 2, 5'-GCTGCCCACTGCATCAG-3'. All gene probes had a double-quenched design, consisting of a 5' FAM fluorophore, an internal ZEN™ (IDT) quencher, and a 3' Iowa Black FQ (IBFQ) quencher. A Step One Plus Real-Time PCR System (Applied Biosystems) was used to perform all qPCR experiments. The β-actin gene was utilized as an endogenous reference against which gene expression levels were standardized. The primer-probe assay for β-actin was as follows: primer 1, 5'-CCTTGCACATGCCGGAG-3'; primer 2, 5'-ACAGAGCCTCGCCTTTG-3'; probe, 5'-TCATCCATGGTGAGCTGGCGG-3'. For relative gene expression, target mRNA levels were normalized to β-actin mRNA levels using

the delta C_T (C_T = cycle threshold) method and the following formula: $2^{-\Delta CT}$ where ΔC_T = target gene C_T – β-actin C_T.

2.4 Gene silencing

All screening siRNA molecules were purchased from IDT, and were designed as 25/27-nucleotide RNA duplexes (Dicer-substrate siRNA). The non-modified screening siRNAs are described in Table 3.1. The modified siARv had the following sequence: sense, 5'-ccAuGcAACUCcUuCaGcAACAGdcdA-3'; antisense, 5'-UGcUGUUGcUgAaGGAGUUGCAuGgug-3'. The siRNA targeting exon 8 of the AR mRNA (siARfl) had the following sequence: sense, 5'-cuGGGAAAGucAAGcccAudTsdT-3'; antisense, 5'-AUGGGCUUGACUUUCCcAGdTsdT-3'. An siRNA targeted against luciferase (siLUC; sense, 5'-cuuAcGcuGAGuAcuucGAdTsdT-3'; antisense, 5'-UCGAAGuACUcAGCGuAAGdTsdT-3') served as a negative control. Alnylam Pharmaceuticals provided the siARfl and siLUC molecules. Lower case letters indicate 2'-O-methyl modification and 's' indicates phosphorothioate RNAs.

For siRNA screening studies, 22Rv1 cells were seeded at 150,000 cells/well in a 24-well plate overnight and treated with the indicated siRNAs using Lipofectamine RNAiMAX (Thermo Fisher Scientific), following the manufacturer's transfection procedure. At the end of the 24 h treatment, cells were lysed for RNA purification and qPCR analysis as described in Section 2.3. For siRNA-LNP-mediated gene knockdown studies, 22Rv1 or LNCaP cells were seeded at 150,000 cells/well overnight in 24-well plates and treated with siRNA-LNP at 0.1 μg/ml siRNA for 24 h (AR knockdown) or 48 h (PSA knockdown). For all gene knockdown studies, the delta-delta C_T method was utilized to calculate relative expression of target mRNAs against a control

reference sample using the following formula: $2^{-\Delta\Delta CT}$ where $\Delta\Delta C_T$ = test sample ΔC_T – control sample ΔC_T.

2.5 Western blot analysis

22Rv1 cells were seeded at 200,000 cells/well overnight in a 12-well plate and transfected with siRNA as described in Section 2.4. After a 48 h treatment, cells were washed with PBS and lysed with RIPA buffer (1% NP-40, 0.25% deoxycholic acid) supplemented with protease inhibitors (Roche Complete Protease Inhibitor Cocktail; Sigma-Aldrich). Aliquots of 10 μg total protein, as quantified by Bradford Assay, were resolved on SDS-PAGE and proteins were transferred to polyvinylidene fluoride membranes. After blocking for 30 min at room temperature in 5% milk in phosphate-buffered saline (PBS)/0.1% Tween-20 (PBS-T), membranes were incubated overnight at 4°C with the indicated primary antibodies and dilutions in PBS-T: AR N-terminus (SC-7305; Santa Cruz Biotechnology, Santa Cruz, CA) at 1:500; AR-V7 (ab198394; Abcam, Cambridge, UK) at 1:500; β-actin (ab8227, Abcam) at 1:5000. β-actin was used as the protein loading control. Following a 45 min incubation with secondary antibody (HRP goat anti-rabbit at 1:20,000 or HRP goat anti-mouse IgG at 1:10,000; Bio-Rad, Hercules, CA) in PBS-T at room temperature, antigen-antibody complexes were detected using Millipore Immobilon Western Chemiluminescent HRP Substrate (Billerica, MA, USA).

2.6 Preparation of siRNA-LNP

All LNPs were prepared at room temperature, using a method as previously described (Kulkarni et al., 2018). Lipids were dissolved in ethanol and mixed together at a molar ratio of 50/10/38.5/1.5 DLin-MC3-DMA, DSPC, cholesterol, and PEG-DMG. For *in vivo* studies, LNP

were prepared using DLin-MC3-DMA, DSPC, cholesterol, and PEG-DSG at molar ratios of 50/10/37.5/2.5. Appropriate volumes of lipid were mixed with siRNA dissolved in 25 mM sodium acetate pH 4 using a microfluidic chip (Precision Nanosystems, Vancouver, BC) or T-junction mixer and a dual-syringe pump (Harvard Apparatus, Holliston, MA). Lipid- and siRNA-containing streams were mixed at a volumetric and flow-rate ratio of 1:3, respectively. Formulations used for *in vitro* studies were formulated at siRNA-to-lipid ratios of 0.056 mg siRNA per μmole lipid, while those used for *in vivo* studies were prepared at 0.028 mg siRNA per μmole lipid. After mixing, the siRNA-LNP systems were then dialyzed twice against 1x PBS pH 7.4 (GIBCO, Carlsbad, CA) using Spectro/Por dialysis membranes (molecular weight cut-off 12,000–14,000 Da, Spectrum Laboratories, Rancho Dominguez, CA). For the biodistribution study requiring radiolabelled LNP, [^{14}C]-DSPC (American Radiolabeled Chemicals, Saint Louis, MO) was incorporated at a ratio of 0.04 μCi/μmol total lipid.

2.7 Analysis of siRNA-LNP

The size (diameter) and polydispersity index (PDI) of LNPs were determined by dynamic light scattering (Malvern Zetasizer Nano ZS, Worcestershire, UK). Total siRNA concentration and siRNA encapsulation was determined by absorbance at 260 nm and by use of the Quant-iT™ RiboGreen™ RNA Assay (Invitrogen). Lipid concentration was derived from measurements of cholesterol content using a Cholesterol E enzymatic assay (Wako Chemicals USA, Richmond, VA). The morphology and size (determined manually by comparing >150 LNPs to the scale bar) of LNP prepared using the T-junction mixing method was determined using cryo-TEM, as described previously (Leung et al., 2012; Kulkarni et al., 2018).

2.8 Cell viability assays

The viability of prostate cancer cells treated with siRNA-LNP was measured using the 3-(4,5-dimethyl-2-thiazolyl)-2,5-diphenyl-2H-tetrazolium bromide (MTT) assay (Sigma-Aldrich), as described previously (Kawamura et al., 2013). Briefly, cells were seeded at 14,000 cells/well (22Rv1 and LNCaP) or 1,500 cells/well (PC3) in 96-well plates, grown overnight, then treated for 96 h with siARv-LNP, siARfl-LNP, or siLUC-LNP at the indicated siRNA concentrations. After 96 h, 25 µl of a 5 mg/ml solution of MTT reagent in PBS was added to cells without aspirating cell media. After a 2 h incubation at 37^{o}C, 100 µl of 20% SDS (w/v) dissolved in 50% dimethyl formamide was added to each well. The absorbance was measured at 570 nm, and values were compared to untreated control to obtain '% cell viability'.

The viability of 22Rv1 cells treated with siRNA-LNP was also determined from attached cell count by Hoechst 33342 (Invitrogen) staining. Cells were seeded at 14,000 cells/well in 96-well plates, grown overnight, and then treated with siARv-LNP, siARfl-LNP, or siLUC-LNP at 1.0 µg/ml siRNA. 100 µl of pre-warmed culture media containing 0.6 µg/ml Hoechst 33342 was added directly to wells at the end of the treatment. Plates were incubated at 37°C for 30 min, then scanned using the Cellomics Arrayscan VTI automated fluorescence imager. The cells were imaged with a 20x objective with the Hoechst channel, and data was collected from 10 fields per well, with three wells per treatment group. A nuclear mask generated by the Cellomics Compartmental Analysis software from the Hoechst stain was used to quantitate cell number. The cell numbers for each treatment were compared to untreated control to obtain '% cell number'.

2.9 Biodistribution of radiolabeled LNP

Male NRG (NOD-*Rag1*^{null} *IL2rg*^{null}) mice were obtained at 6 to 10 weeks of age. After 1 week of adaptation, mice were inoculated subcutaneously with $2x10^6$ 22Rv1 cells suspended in 50% Matrigel on the lower back under isoflurane anesthesia. Tumor dimensions were measured externally with calipers beginning when palpable, and tumor volumes were calculated according to the following equation: $(\text{length} \times \text{width})^2/2$, with the length (mm) being the longer axis of the tumor. When tumor size reached 250 mm^3, siARv-LNP containing trace amounts of [^{14}C]-DSPC were administered by a single injection of 5 mg siRNA/kg body weight into the lateral tail vein at an injection volume of 10 µl/g mouse. At 24 h, the mice were anesthetized with CO_2 and blood withdrawn by cardiac puncture for collection in microtainer tubes with EDTA (Becton-Dickinson, Franklin Lakes, NJ). A portion of the blood was centrifuged at 500 x *g* for 10 min to isolate plasma. Tumor and organ tissues were processed by transferring the pre-weighed whole organs (or a piece of the liver, 40-60 mg) to Fastprep tubes and homogenized in PBS (0.75–1 ml) using a Fastprep-24 (MP Biomedical, Santa Ana, CA). Aliquots (0.1–0.2 ml) of the homogenate and plasma were transferred to 7 ml glass scintillation vials and subjected to a digestion and decolorization protocol as previously described (Mui et al., 2013). Radioactivity was measured using a Beckman Coulter LS 6500 liquid scintillation counter (Mississauga, Ontario, Canada). The percent recovery in blood was calculated based on a blood volume of 70 ml/kg body weight (Mui et al., 2013). Tumor and organ associated radioactivity are expressed as percent injected dose per total organ weight.

2.10 *In vivo* efficacy study

Male NRG mice were inoculated with 22Rv1 cells as described in section 2.9. When tumor size reached 100 mm^3, mice were randomly assigned to PBS control or 5 mg/kg siARv-LNP, siARfl-LNP or siLUC-LNP (11 mice per group) at an injection volume of 10 µl/g mouse. The initial tumor volumes before injection were not significantly different among the 4 groups (P=0.7366). The average tumor volume relative to treatment day 0 for each group, as measured with calipers throughout the study, as well as the number of biological replicates, can be found in Appendix A. Mice were treated intravenously through the lateral tail vein once daily for 3 days and then twice per week thereafter. Surviving mice were sacrificed on treatment day 20. Tumors were harvested, snap frozen in liquid nitrogen, and stored at -80° until further processed for evaluation of mRNA expression by qPCR. One mouse from the siARfl-LNP treatment group was found dead prematurely on treatment day 10, and was removed from the study.

2.11 RNA isolation from xenograft tissue

A piece of each tumor tissue was transferred to a Fastprep tube and homogenized in 0.75 ml TRIzol reagent (Thermo Fisher Scientific) using a Fastprep-24 instrument. RNA was then isolated from the homogenized samples following the TRIzol reagent procedural guidelines. To begin, the lysate was centrifuged for 5 min at 12,000 x *g* at 4 °C. After a 5-min incubation at room temperature, 0.15 ml of chloroform was added before another incubation for 3 min at room temperature. After centrifuging the sample for 15 min at 12,000 x *g* at 4 °C, the aqueous phase was transferred to a new tube. To precipitate the RNA, 0.375 ml of cold isopropanol was added to the sample, incubated for 10 min, then centrifuged for 15 min at 12,000 x *g* at 4 °C. After discarding the supernatant, the pellet was resuspended in 0.75 ml of 75% ethanol, vortexed for

10 sec, then centrifuged for 5 min at 7,500 x *g* at 4 °C. The supernatant was discarded, and the pellet was allowed to air dry for 10 min before resuspending in RNase-free water. A NanoDrop™ Lite Spectrophotometer was used to determine total RNA concentrations, and 1 µg of total RNA was used as template for cDNA synthesis, and qPCR experiments were carried out as described in Section 2.3.

2.12 Statistical analysis

Student's t-test or one-way ANOVA were used to assess significance of differences among treatment groups. The log-rank test was applied to analyze survival data. All statistical analysis was performed using Graph Pad Prism 6 software. Levels of statistical significance were set at $P<0.05$.

Chapter 3: Results

3.1 Expression of androgen receptor variants in prostate cancer cell culture models

The main objective of this body of work was to design an siRNA-LNP system that could target all forms of the AR, a key transcription factor in the growth and survival of prostate cancer. Figure 3.1 illustrates the structural differences between wild-type/full-length AR, and mutant or variant ARs, and describes how a strategically designed siRNA molecule could target all variations. The wild-type or full-length AR mRNA is composed of 8 exons, which code for the NTD, the DBD, the hinge region, and the LBD (Figure 3.1 A). Most of the anti-androgen therapy in the clinic targets the LBD of the AR, and is inefficient at targeting those ARs with mutations in the LBD (Figure 3.1 B) or constitutively active splice variant ARs which completely lack the LBD, such as AR-V7 (Figure 3.1 C). AR-V7 mRNA contains exons 1 to 3, and the variant-specific cryptic exon 3 (CE3). Although a number of AR splice variants have been characterized, the AR-V7 splice variant has a relatively high expression frequency and abundance, as well as high detection rates in late-stage prostate cancer (Sharp et al., 2019). Previous studies carried out by the Cullis laboratory have tested the effects of siRNA-LNP systems targeting full-length AR mRNA only – siRNA designed against exon 8 (siARfl) (Lee et al., 2016). By designing an siRNA molecule against exon 1 of the AR gene, the expression of full-length AR, AR with mutations in the LBD, and splice variant ARs could be affected; thus, providing a more universal anti-AR therapeutic approach.

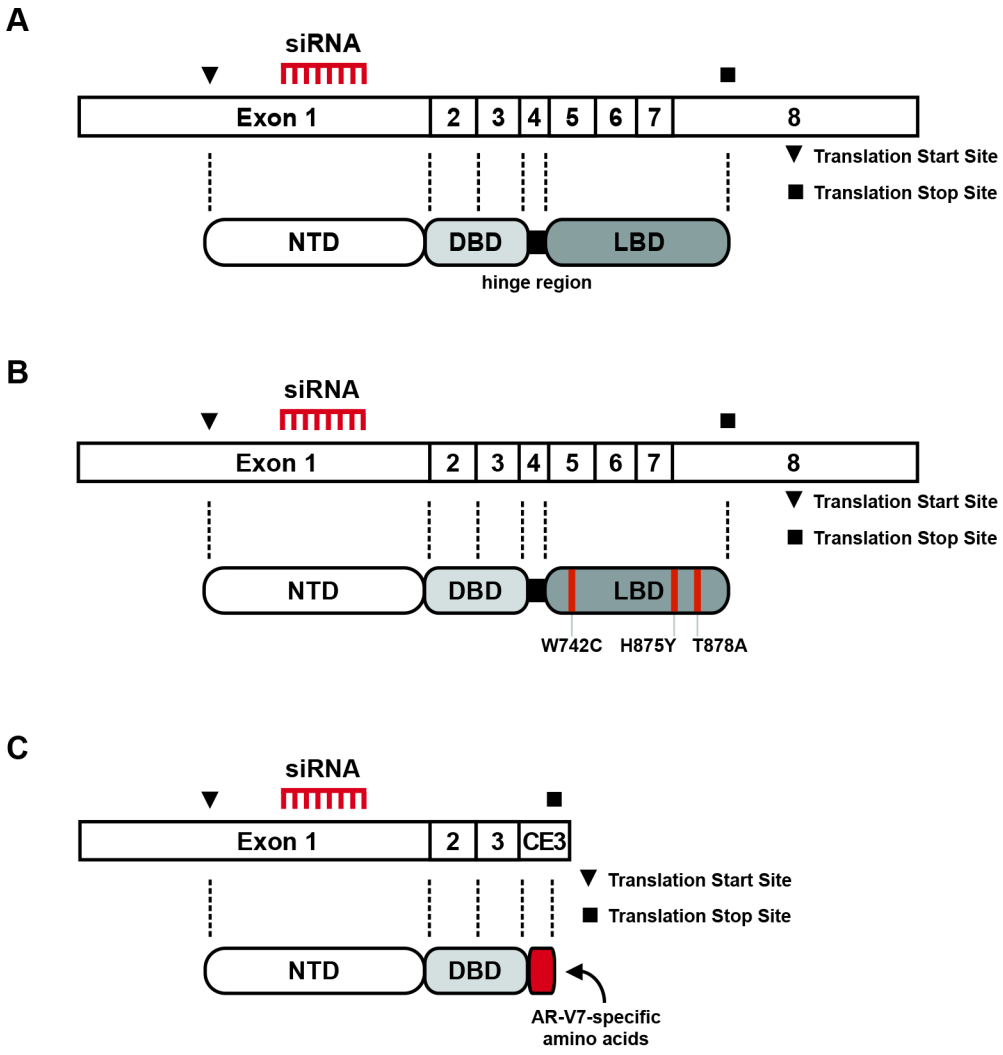

Figure 3.1 Targeting exon 1 of wild-type and variant androgen receptor mRNA with siRNA.

Using endogenous RNA interference machinery, siRNA-mediated gene silencing can affect the expression of a broad AR population. This includes (**A**) full-length AR, (**B**) AR with mutations in the LBD that confer promiscuous steroid signaling and anti-androgen antagonism, and (**C**) constitutively active AR splice variants that completely lack the LBD, such as AR-V7 (CE3 splicing results in 16 variant-specific amino acids at the C-terminus).

To facilitate the optimization of a ubiquitous siRNA-LNP system targeting all AR variants, studies were to be performed in prostate cancer model systems with differing AR molecular phenotypes. The 22Rv1 and LNCaP cell lines were chosen as those model systems, as previous studies have collectively concluded that they exhibit varying degrees of expression and dependency for the AR and AR-V7 genes (Guo et al., 2009; L. Liu & Dong, 2014). Before functional assays were carried out in the laboratory using these cell lines, the mRNA expression levels of AR and AR-V7 were confirmed for 22Rv1 and LNCaP cells. RNA was extracted from untreated cells under normal growth conditions (RPMI-1640 supplemented with 10 % FBS), utilized as template for cDNA synthesis, and analyzed by qPCR using the gene assays described in Section 2.3. The cycle threshold (C_T) for each target gene was normalized to that of the β-actin gene using the delta C_T method, and represented as relative mRNA expression values (Figure 3.2). The 22Rv1 cell line, derived from a castration-resistant xenograft of human prostate cancer cells (Sramkoski et al., 1999), was confirmed to have comparable levels of AR mRNA and relatively high endogenous levels of the splice variant AR-V7 (Figure 3.2 A), compared to that of the LNCaP cell line (Figure 3.2 B). This relatively enhanced expression level of AR-V7 in the 22Rv1 model is likely a result of the intragenic duplication of a region encompassing exon 3, and its promotion of alternative splicing and incorporation of alternative exons preceding exon 4 (Li et al., 2011). As shown by Figure 3.2 B, the LNCaP cell line, a human androgen-dependent cell line derived from a lymph metastasis (Horoszewicz et al., 1983), exhibited relatively lower expression levels of AR-V7 mRNA. This is in agreement with previous studies reporting that LNCaP cells express extremely low levels of AR-V7 mRNA, and do not express detectable levels of the AR-V7 protein (Guo et al., 2009; L. Liu & Dong, 2014). The expression levels of PSA mRNA relative to that of β-actin for 22Rv1 and LNCaP cells are

also shown in Figure 3.2. The promoter of the PSA gene includes several binding sites for the AR, and activation of the AR leads to transcription and translation of PSA (Cleutjens et al., 1996). AR-V7 has also been shown to occupy the PSA promoter and upregulate it expression (Cao et al., 2014). For this reason, PSA levels serve as an index for impacting signaling by ARs. Taken together, the 22Rv1 and LNCaP cells, with low to high levels of AR splice variant expression, mimic the variation of AR status in the clinic, and are useful models to test the efficacy of AR-targeted siRNA-LNP systems on cells.

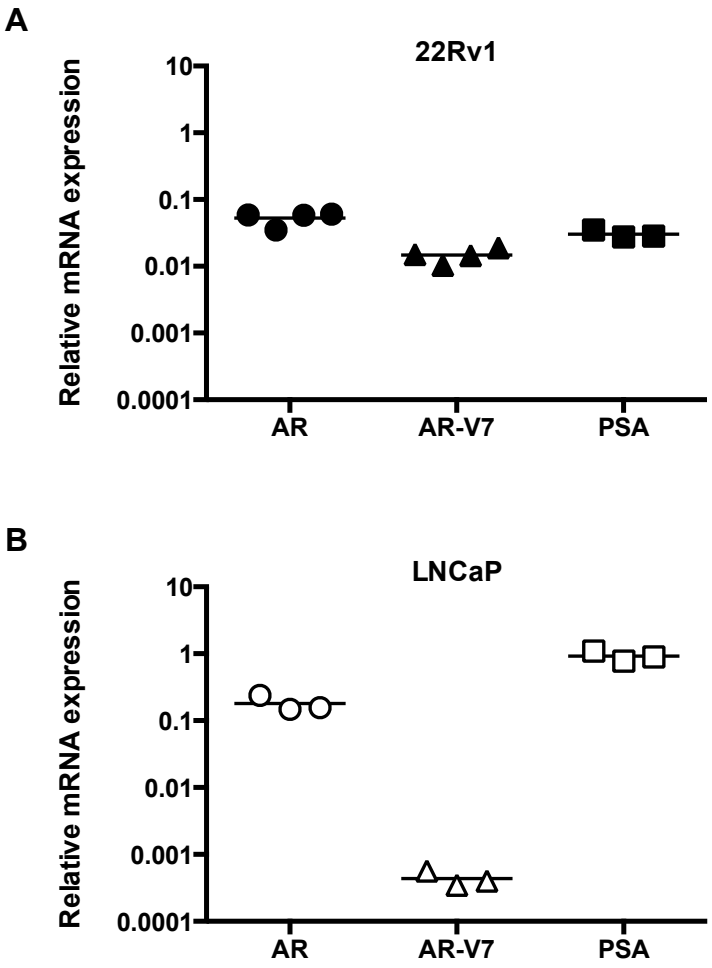

Figure 3.2 Relative expression of AR, AR-V7, and PSA mRNA in prostate cancer cell culture models.

C_T values from qPCR analysis of AR, AR-V7, and PSA mRNA were normalized to that of β-actin and expressed as relative mRNA expression values for untreated cells. (**A**) The 22Rv1 cell line is positive for AR and PSA mRNA, with relatively high endogenous expression of the AR-V7 splice variant. 22Rv1 cells model prostate cancer with a mixed population of full-length and splice variant ARs. (**B**) The LNCaP cell line, the dominant model in prostate cancer research, expresses high levels of AR and PSA mRNA, and extremely low levels of the AR-V7 splice variant mRNA. Symbols represent biological replicates; mean values are represented by horizontal bar.

3.2 Selection of an siRNA sequence for efficient knockdown of ARs

To begin the process of identifying a potent AR-targeted siRNA, a total of five screening siRNA molecules were designed by IDT against AR exon 1. The sequences of the screening siRNA are shown in Table 3.1, and the respective alignments within the AR mRNA (NM_000044) are shown in Figure 3.3. The knockdown efficiencies of the screening siRNAs were tested *in vitro* in 22Rv1 cells using a commercial transfection reagent, Lipofectamine RNAiMAX. After 24 h of treatment with 10 nM siRNA, the relative AR and AR-V7 mRNA knockdown efficiencies of the siRNA sequences were compared by qPCR. All five siRNA sequences were capable of significantly reducing mRNA levels of both AR and AR-V7 relative to the untreated control (Figure 3.4 A). It is encouraging that the different siRNAs targeting AR exon 1 produced a similar trend in mRNA knockdown, that is treatment with all sequences reduced AR and AR-V7 mRNA levels to a certain degree. This is supporting evidence that unsuspected sequence-specific off-target effects are not creating the exhibited gene knockdown results. AR and AR-V7 knockdown efficiency of the screening molecules was compared to that of an siRNA designed against exon 8 of the AR gene, siARfl (Section 2.4). This siRNA was previously tested in the LNCaP model, showing effective knockdown of full-length AR *in vitro*, as well as in LNCaP xenografts following repeat dosing (Lee et al., 2016). Treatment with siARfl resulted in efficient reduction of full-length AR mRNA levels, but did not greatly reduce levels of AR-V7 mRNA in 22Rv1 cells, compared to the control treatments. This siRNA molecule would serve as a phenotypic control for knockdown of full-length AR only. The siRNA targeting the luciferase gene (siLUC) served as an effective negative control, as treatment with this molecule significantly affected neither AR nor AR-V7 mRNA levels relative to the untreated control.

Based on the knockdown activity of the screening siRNA molecules, the most potent AR exon 1-targeted sequence, siARv, was selected for modification and retested in 22Rv1 cells to confirm that mRNA knockdown would not be affected by the altered siRNA chemistry. Methylation of the 2'-OH at specific sites of siRNA has been shown to enhance stability and persistence of RNA interference (Behlke, 2008). Incorporation of 2'-O-Me RNA residues into siRNA molecules can also prevent activation of the innate immune system and is an important factor in designing potent siRNA formulations (Judge et al., 2006). A standard IDT 2'-O-Me modification was introduced into the siARv sequence (Section 2.4) and tested against control siRNA molecules in 22Rv1 cells, as was carried out with the screening siRNA. The sequence showed equally efficient gene knockdown activity after introducing the modification (Figure 3.4 B), ~70% knockdown of AR mRNA and ~85% reduction in AR-V7 mRNA expression, and was therefore selected for use in all subsequent studies.

The levels of full-length AR, LBD-truncated AR, and AR-V7 protein after treatment with all screening and modified siRNAs were also measured. 22Rv1 cells were transfected with 10 nM of the siRNA described using Lipofectamine RNAiMAX, and treated for 48 h. Protein extracts were separated by SDS-PAGE and western blot analysis was used to measure levels of AR and AR variant protein by an AR N-terminal-targeted antibody, as well as levels of AR-V7 protein by an AR-V7-specific antibody (Figure 3.4 C). β-actin protein was used as a loading control. The results show that the siARv-mediated effects seen on mRNA levels were ultimately mirrored in protein levels. Mainly, treatment with siARv resulted in the most efficient and persistent knockdown of full-length and variant AR protein, as well as AR-V7 protein. Incorporation of the 2'-O-Me modifications in the siARv molecule did not reduce protein knockdown of ARs compared to that of the non-modified siARv. Treatment with siARfl only

greatly reduced levels of full-length AR, while the negative control siLUC did not seemingly affect levels of any ARs. For all subsequent experiments, siARv will refer to the 2'-O-methylated siARv molecule.

Name	Sequence
siARv	Sense: 5'-CCAUGCAACUCCUUCAGCAACAGdCdA-3'
	Antisense: 5'-UGCUGUUGCUGAAGGAGUUGCAUGGUG-3'
siARv- β	Sense: 5'-CACUUCCUCCAAGGACAAUUACUdTdA-3'
	Antisense: 5'-UAAGUAAUUGUCCUUGGAGGAAGUGGG-3'
siARv- γ	Sense: 5'-GGAAAGCGACUUCACCGCACCUGdAdT-3'
	Antisense: 5'-AUCAGGUGCGGUGAAGUCGCUUUCCUG-3'
siARv- δ	Sense: 5'-GGAUAGCUACUCCGGACCUUACGdGdG-3'
	Antisense: 5'-CCCGUAAGGUCCGGAGUAGCUAUCCAU-3'
siARv- ε	Sense: 5'-GACCUUAAAGACAUCCUGAGCGAdGdG-3'
	Antisense: 5'-CCUCGCUCAGGAUGUCUUUAAGGUCAG-3'

Table 3.1 Sequences of screening siRNA molecules.

Five siRNA sequences targeting exon 1 of AR mRNA were designed by Integrated DNA Technologies (IDT). 'd' indicates DNA bases.

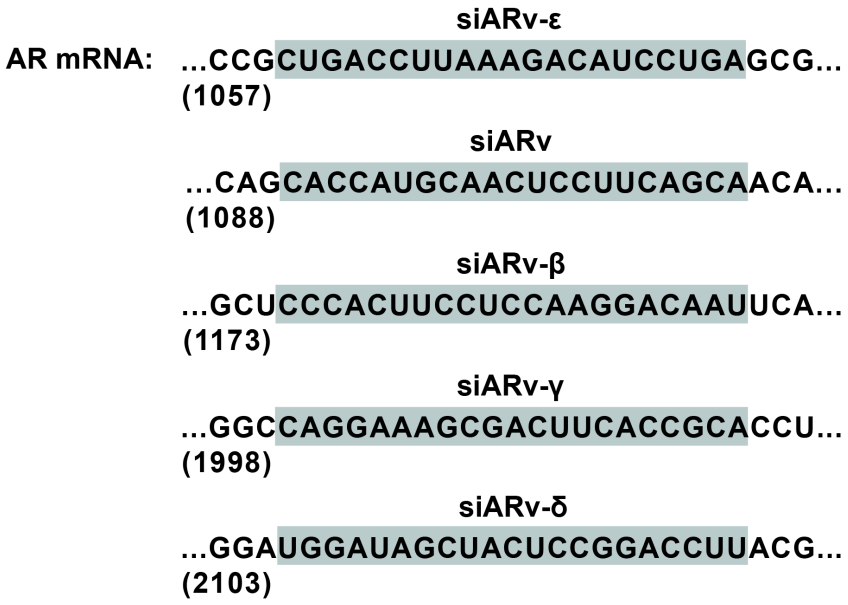

Figure 3.3 Final target sequence of each screening siRNA within the AR mRNA (accession number NM_000044).

A

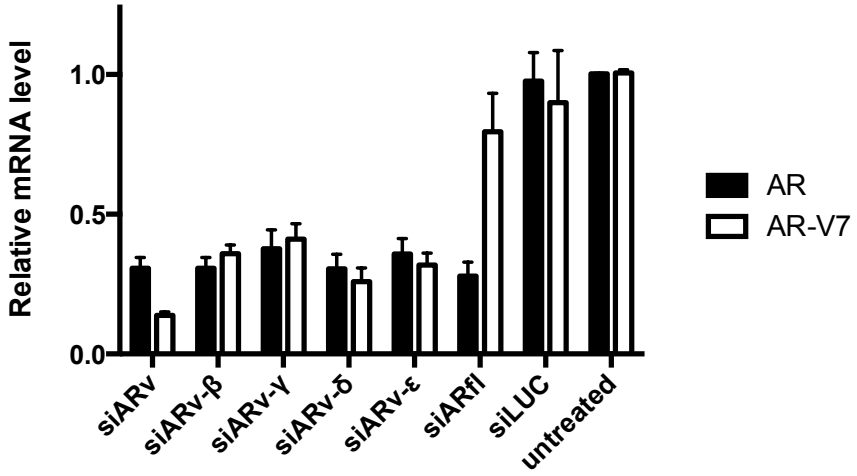
Relative mRNA level
1.0
0.5
0.0
siARv
siARv-β
siARv-γ
siARv-δ
siARv-ε
siARfl
siLUC
untreated
AR
AR-V7

B

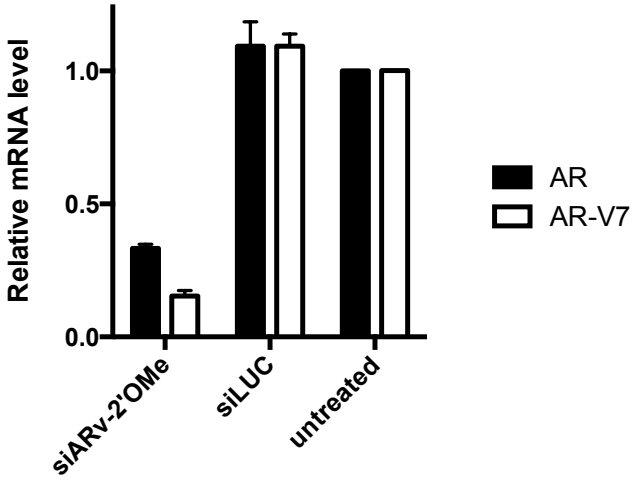
Relative mRNA level
1.0
0.5
0.0
siARv-2'OMe
siLUC
untreated
AR
AR-V7

C

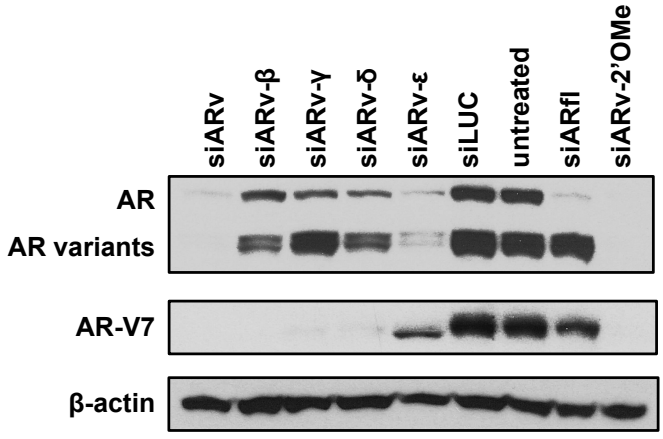
siARv
siARv-β
siARv-γ
siARv-δ
siARv-ε
siLUC
untreated
siARfl
siARv-2'OMe
AR
AR variants
AR-V7
β-actin

Figure 3.4 Optimizing an siRNA targeting AR variants in 22Rv1 cells.

(**A**) 22Rv1 cells were transfected with siRNA targeted against exon 1 of the AR mRNA (siARv, siARv-β, siARv-γ, siARv-δ, or siARv-ε) using Lipofectamine RNAiMAX and 10 nM siRNA. Knockdown efficiency was compared to siRNA targeting the exon 8 of AR mRNA (siARfl) and negative control siRNA complementary to the luciferase gene (siLUC). RNA was purified from cells at 24 h post-transfection. Data represents mean mRNA level relative to untreated control (± SD); n=4. (**B**) 22Rv1 cells were transfected as in panel A with 2'-O-methylated siARv or siLUC control. Data represents mean mRNA level relative to untreated control (± SD); n=3. (**C**) 22Rv1 protein lysates prepared 48 h post-transfection were analyzed for full-length and variant AR expression (by the AR N-terminus antibody), as well as AR-V7 expression (by the AR-V7 specific antibody). The detection of β-actin expression was performed to monitor protein loading.

3.3 LNP-mediated delivery of siARv leads to efficient knockdown of ARs and PSA in prostate cancer cell models

Once the siARv molecule was identified through small-scale screening efforts, the molecule was formulated into LNP systems in order to confirm the knockdown efficiency in both 22Rv1 and LNCaP models, as well as to perform *in vitro* functional assays. LNPs utilized for all *in vitro* studies were formulated with the ionizable amino lipid, DLin-MC3-DMA, and the PEG-lipid, PEG-DMG, a formulation that is optimized for siRNA delivery and silencing in hepatocytes (Jayaraman et al., 2012). Figure 3.5 shows a representative cryo-TEM image of LNP encapsulating siARv. The LNP systems exhibited the expected electron-dense core structure, which is proposed to primarily contain siRNA and ionizable amino lipid (Leung et al., 2012; Kulkarni et al., 2018). The apparent size of the LNP system agreed with measurements derived from dynamic light scattering, which measured the prepared systems at ~50 nm. Mainly, the LNP size depicted by the cryo-TEM imaging was 50 ± 10 nm, as expected with systems containing a molar content of 1.5% PEG lipid (Chen et al., 2016; Kulkarni et al., 2018).

In order to confirm that the siARv molecule in the LNP carrier was capable of targeted gene knockdown, 22Rv1 and LNCaP cell lines were treated with siRNA-LNP at 0.1 μg/ml siRNA, which corresponds to ~6 nM siRNA, for 24 h and assayed for the effects on gene expression. AR and AR-V7 mRNA levels relative to the untreated control were measured by qPCR using the delta-delta C_T method. LNP carrying siARv mediated specific knockdown of AR and AR-V7 mRNA in both cell lines (Figure 3.6). In agreement with the siRNA screening studies, LNP containing siARfl demonstrated an ability to greatly reduce AR mRNA levels, and not those of AR-V7 mRNA. Treatment with LNP containing the control siLUC did not mediate knockdown of AR mRNAs, further highlighting the specificity of the siARv molecule as well as

the LNP carrier itself, under the specific experimental parameters. The overall potency of the DLin-MC3-DMA-LNP system in cell culture shows greater potency than Lipofectamine RNAiMAX (Figure 3.4 A), and is comparable to that seen in prostate cancer cells for siRNA-LNP systems targeting an alternative gene, clusterin (Yamamoto et al., 2015a).

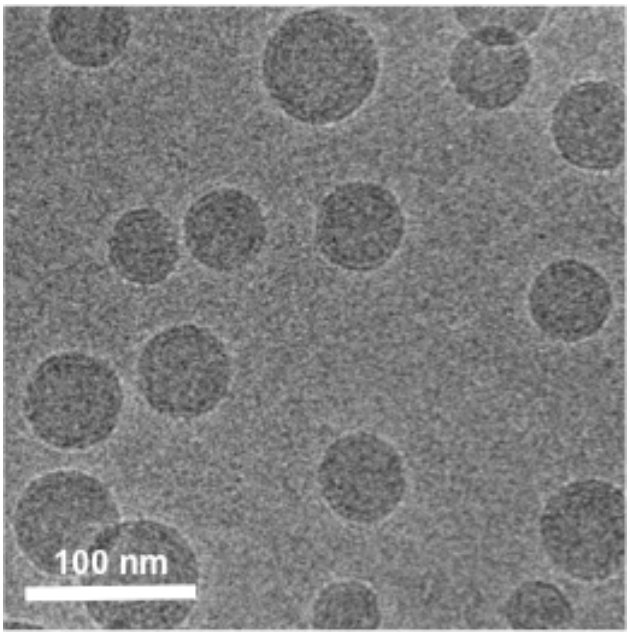

Figure 3.5 Representative cryo-TEM image of DLin-MC3-DMA-containing LNP formulated with siARv.

The micrograph of LNP prepared with a T-junction mixer shows the expected solid-core structure and diameter of 50 ± 10 nm. Scale-bar represents 100 nm.

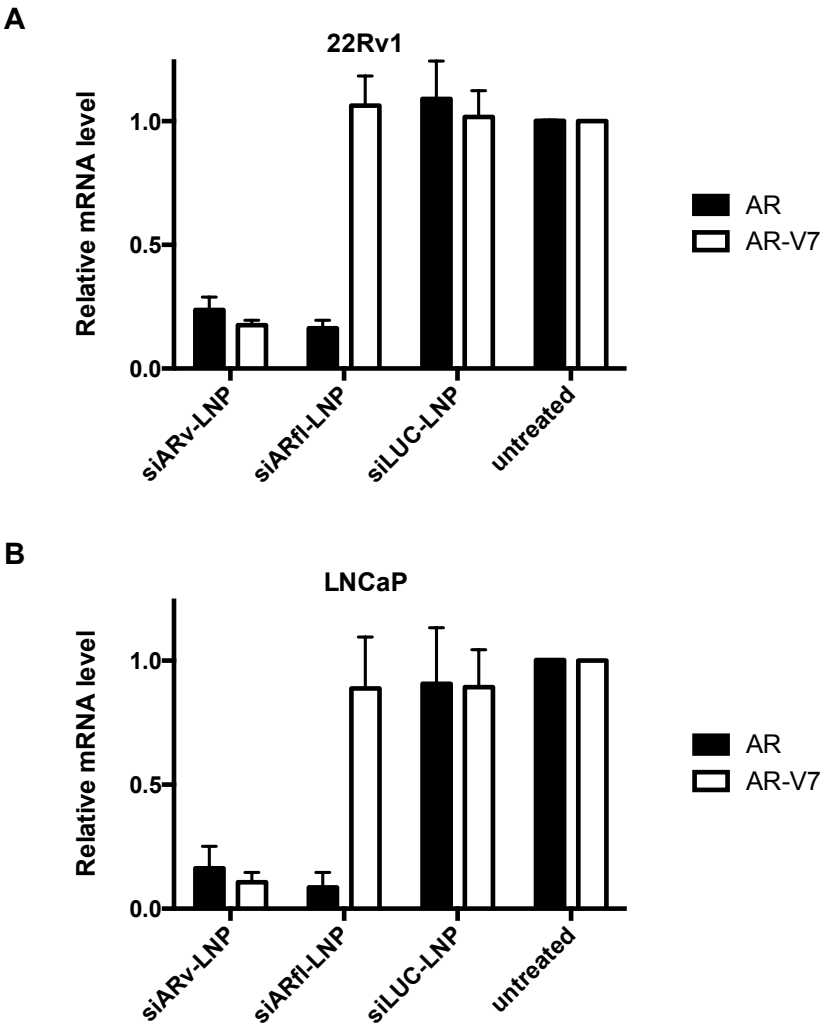

Figure 3.6 Encapsulation of siARv in DLin-MC3-DMA-containing LNP mediates *in vitro* knockdown of AR and AR-V7 mRNA in prostate cancer cells.

AR and AR-V7 mRNA expression levels were detected in (**A**) 22Rv1 and (**B**) LNCaP cells following treatment with 0.1 μg/ml siARv-LNP, siARfl-LNP, or siLUC-LNP for 24 h. Expression of each gene was normalized to the β-actin gene. Data represents mean mRNA level relative to untreated control (± SD); n=4.

In order to begin determining the functional effects of treatment with siARv-LNP, and the resulting knockdown of wild-type and variant ARs, attention was focused to measuring the AR transcriptional activity in 22Rv1 and LNCaP cells. In order to assess the degree of AR function, transcriptional activity was derived from the levels of PSA mRNA expressed by the prostate cancer cells. Treatment with siARv-LNP at 0.1 μg/ml siRNA for 48 h showed a significant reduction in PSA expression in both 22Rv1 and LNCaP cell lines relative to the siLUC-LNP and untreated controls (Figures 3.7). By contrast, siARfl-LNP was only effective in reducing PSA mRNA levels in LNCaP cells under the treatment conditions (Figure 3.7). This result corresponds to the negligible amount of variant ARs expressed in the LNCaP cell line, and the fact that full-length AR mediates the majority of AR transcriptional activity; whereas, the 22Rv1 cell line expresses high endogenous levels of variant ARs, specifically of AR-V7, which can interact with PSA promoter regions and mitigate the effect of full-length AR knockdown on AR signaling. The results are in agreement with previous AR-regulated transcriptome studies, where treatment with an antisense oligonucleotide (ASO) targeting exon 8 of AR mRNA did not reduce 22Rv1 levels of PSA mRNA, but did so in an LNCaP-derived cell line (Yamamoto et al., 2015b). These data indicate that LNP containing siARv are capable of inhibiting AR signaling in prostate cancer cell models with differing AR variant expression and dependence, and thus have a broader application than the siARfl-LNP system.

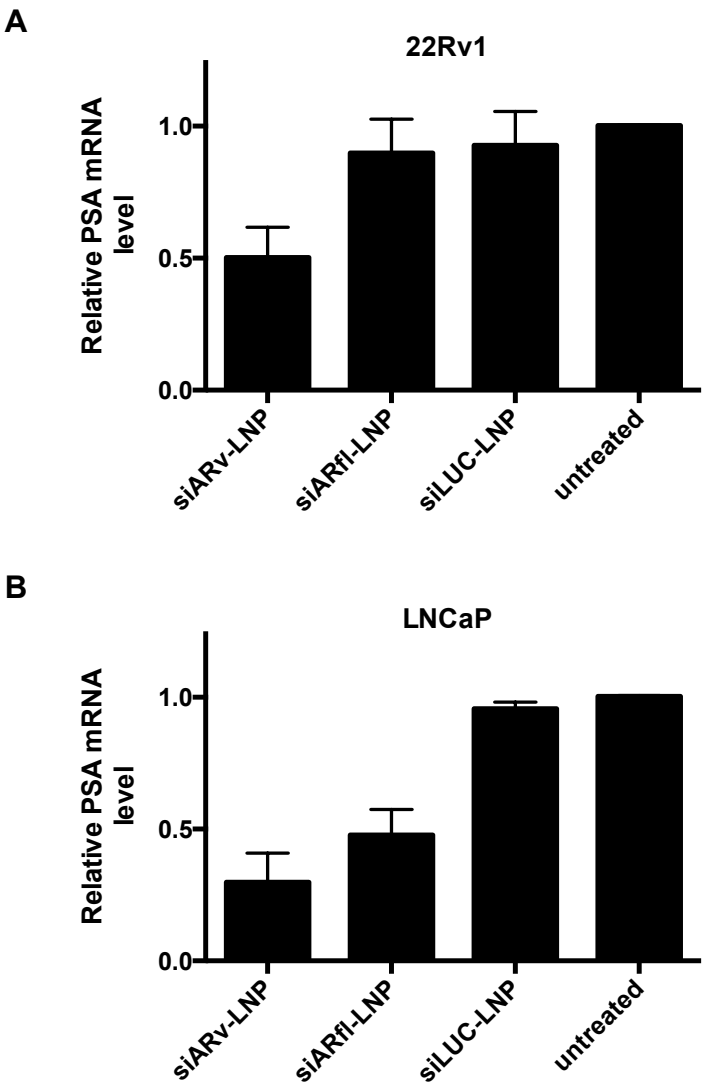

Figure 3.7 Treatment with siARv-LNP decreases PSA mRNA expression levels in both 22Rv1 and LNCaP cells *in vitro*.

PSA mRNA expression levels were detected in (**A**) 22Rv1 and (**B**) LNCaP following treatment with 0.1 μg/ml siARv-LNP, siARfl-LNP, or siLUC-LNP for 48 h. Expression under all treatments was normalized to the β-actin gene. Data represents mean mRNA level relative to untreated control (± SD); n=3.

3.4 Effects of siARv-LNP on cell viability *in vitro*

After confirming the functional knockdown of ARs by the siARv-LNP system, as exhibited by the reduction of AR-mediated PSA gene expression, the effects on cell viability were tested. Prostate cancer cells were treated with LNP containing siARv, siARfl, or siLUC at concentations of 0.1, 1.0, and 10 μg/ml siRNA for 96 h. At the end of the treatment, MTT reagent was added to the cells and a measure of cell mitochondrial activity was derived from the fluorescence of formazan, a metabolic product of the reagent. All fluorescence values were normalized to the untreated control, and represented as a percentage of cell viability. Treatment with 1.0 μg/ml siARv-LNP reduced cell viability by 40-60% in 22Rv1 and LNCaP cells (Figure 3.8 A and B, respectively). It is important to note that siARv-LNP more potently suppressed cell growth compared with siARfl-LNP in 22Rv1 cells, in agreement with the significant role for variant ARs in this cell line (Yamamoto et al., 2015b). This previous study compared ASOs targeting exon 1 and exon 8 of the AR mRNA; here, they were also able to show that 22Rv1 is more responsive to treatment with exon 1-targeted ASO and suggesting a significant role of variants ARs in this specific model. In LNCaP cells, siARv-LNP and siARfl-LNP both reduced cell viability and there was no significant difference between their effects. These results indicate that targeting exon 1 of the AR gene, and thus knocking down both full-length and variant AR, is effective across cell lines with different AR expression profiles and androgen dependency. It also indicates that knockdown of full-length AR alone with the siARfl-LNP system, and antagonizing full-length AR signaling as is routine in the clinical setting, is not an effective treatment for those prostate cancer models with increased expression and dependence of AR splice variants, such as the 22Rv1 model. LNP containing AR exon 1-targeted siRNA had no significant effect on viability of PC3 cells, which do not express functional ARs (Figure 3.8 C).

These data support the notion that the siARv molecule is specific to AR mRNAs, and does not affect prostate cancer cell growth and survival that is independent from ARs. Similarly, treatment with LNP containing siARfl and siLUC did not significantly affect cell viability relative to the untreated control in the AR-negative PC3 cell line (Figure 3.8 C).

It is important to note that of the three cells lines tested, 22Rv1 cell viability is particularly affected by treatment with increasing concentrations of siLUC-LNP, a system which should not exhibit targeted effects on cell viability. Treatment with another negative control siRNA targeting the GAPDH gene has been shown to exhibit a similar reduction in 22Rv1 cell viability (data not shown), indicating that it is likely a non-specific effect of the LNP system itself causing this reduction in cell viability.

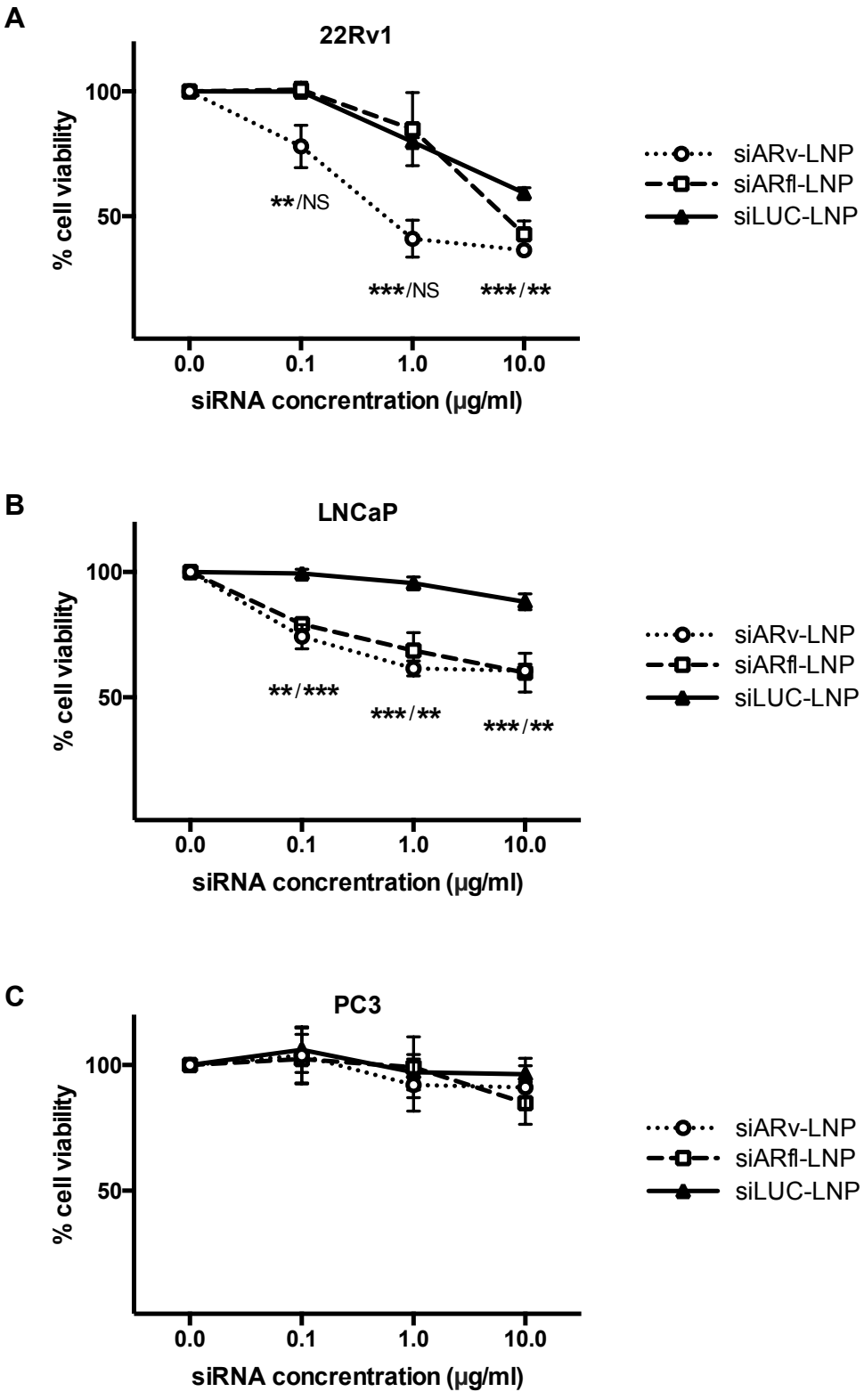
A
22Rv1
100
50
% cell viability
**/NS
***/NS
***/**
0.0
0.1
1.0
10.0
siRNA concrentration (µg/ml)
siARv-LNP
siARfl-LNP
siLUC-LNP
B
LNCaP
100
50
% cell viability
/*
***/**
***/**
0.0
0.1
1.0
10.0
siRNA concrentration (µg/ml)
siARv-LNP
siARfl-LNP
siLUC-LNP
C
PC3
100
50
% cell viability
0.0
0.1
1.0
10.0
siRNA concrentration (µg/ml)
siARv-LNP
siARfl-LNP
siLUC-LNP

Figure 3.8 Treatment with siARv-LNP reduces viability of both 22Rv1 and LNCaP cell cultures, as measured by MTT assay.

MTT assay was used to evaluate effects of siARv-LNP, siARfl-LNP, and siLUC-LNP on viability in (**A**) 22Rv1, (**B**) LNCaP, and (**C**) PC3 cells (AR negative) following a 96 h treatment. Results are expressed as percentage absorbance at 570 nm relative to the untreated control cells. Data represents mean ± SD; n=3-4. ***P<0.001, **P<0.01 or *P<0.05 siARv-LNP/siARfl-LNP compared with siLUC-LNP control.

The effect of siARv-LNP on 22Rv1 cell viability was also determined by high throughput fluorescence imaging. Here, the viability was derived from attached cell number, as opposed to the overall mitochondrial activity that was measured by the MTT assay. First, 22Rv1 cells were seeded overnight in a 96-well plate. After treatment with LNP at 1.0 μg/ml siRNA for 96 h, live cells were stained with a cell-permeable Hoechst dye, and analyzed using the Cellomics Arrayscan VTI automated fluorescence imager. The attached cell count for each treatment was derived from the total number of Hoechst-stained nuclei from three plate wells (10 fields per well), and represented as the percentage of cells relative to the untreated control. Treatment with LNP carrying siARv resulted in a significantly lower 22Rv1 cell number over siLUC-LNP and the untreated control after 96 h of treatment (Figure 3.9 A). As exhibited with the cell viability measurements of the MTT assay in Figure 3.8 A, treatment with 1.0 μg/ml siARfl-LNP had no significant effect on 22Rv1 cell viability compared to the siLUC-LNP control. 22Rv1 cells also exhibited a higher degree of morphological changes in the nuclei typical of apoptosis (condensed and fragmented nuclei), as indicated by the representative fluorescence images shown in Figure 3.9 B. Together, the cell viability observations indicate that the siARv-LNP system has a broader prostate cancer treatment application than siRNA-LNP systems targeting full-length AR alone. Specifically, the results from *in vitro* studies indicate that siARv-LNP should be carried forward and tested as a therapy for 22Rv1-derived tumors *in vivo*.

A

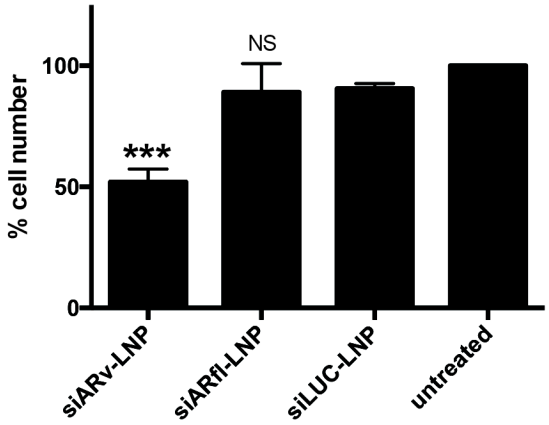
NS
100
***
% cell number
50
0
siARv-LNP
siARfl-LNP
siLUC-LNP
untreated

B

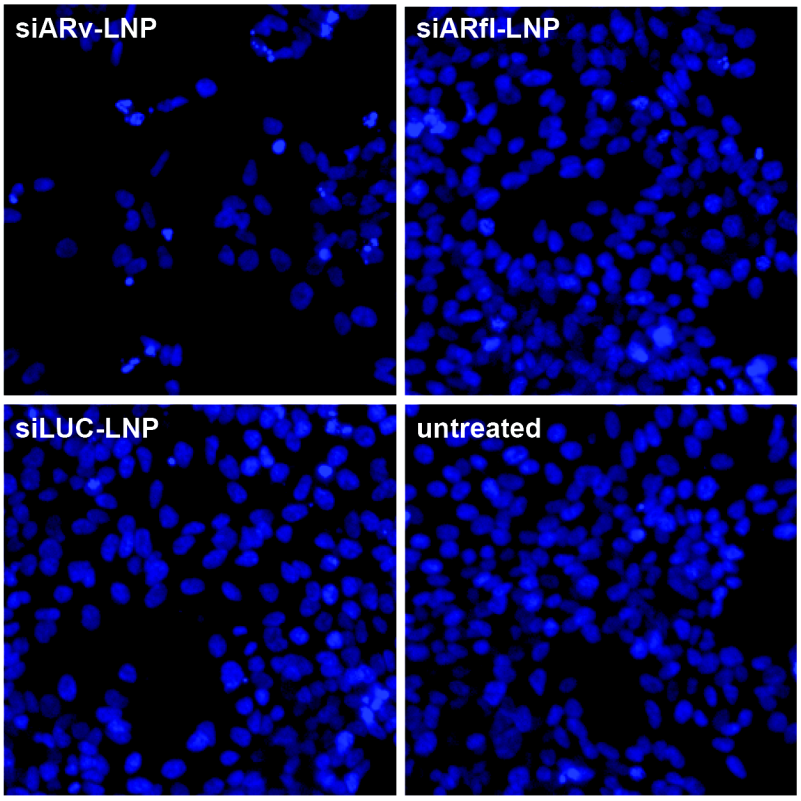
siARv-LNP
siARfl-LNP
siLUC-LNP
untreated

Figure 3.9 Treatment with siARv-LNP reduces 22Rv1 cell viability, as measured by high throughput fluorescence imaging.

(**A**) 22Rv1 cells were treated with 1.0 μg/ml siARv-LNP, siARfl-LNP, or siLUC-LNP for 96 h. After staining with Hoechst 33342 (blue), cell number was detected by a Cellomics Arrayscan VTI automated fluorescence imager (10 fields per well, three wells per treatment). Results are expressed as a percentage of cell number relative to the untreated control. Data represents mean ± SD; n=3 individual experiments. (**B**) Representative images of 22Rv1 cells exposed to the indicated treatments.

3.5 Biodistribution of siARv-LNP in mice bearing 22Rv1-derived xenografts

Prior to testing the *in vivo* efficacy of the siARv-LNP system, the biodistribution properties were determined for a system formulated with trace amounts of radiolabeled lipid, [^{14}C]-DSPC. Previous studies had compared tumor accumulation between differing LNP formulations (Lee et al., 2016), but the biodistribution of these systems in a xenograft tumor model had yet to be determined. In addition, the biodistribution of these systems had yet to be determined at a dose comparable to those utilized for treating prostate cancer-derived xenografts. Earlier studies carried out by the Cullis laboratory have demonstrated that the dissociation rate of DSPC from systems of a similar size is less than 1% per hour in mouse plasma, making radiolabeled DSPC a viable LNP tracker lipid (Chen et al., 2016). For the LNP systems utilized *in vivo*, the PEG lipid anchor was altered, and the PEG lipid density and ratio of lipid to siRNA in the LNP were both increased. Previous studies have shown that utilizing a PEG lipid with longer anchoring alkyl chains (PEG-DSG with stearyl chains as opposed to PEG-DMG containing myristoyl chains) increases the circulation life-time of the system (Chen et al., 2016), which could increase the amount of LNP that reaches the distal tumor site. In addition, improved *in vivo* gene silencing potency has been observed upon increasing the LNP lipid-to-siRNA ratio twofold for systems with a similar PEG lipid content (Chen et al., 2016). A ratio of 0.028 mg siRNA per μmole lipid has shown maximal *in vivo* potency with a hepatocyte target, FVII, and so was utilized for all *in vivo* studies described in this thesis.

Male NRG mice bearing 22Rv1 xenografts were intravenously injected with siARv-LNP 5 mg siRNA/kg body weight once tumors reached 250 mm^3, as determined by external caliper measurements. After 24 h of treatment, the accumulation of radiolabel was measured in tumor tissue and blood, as well as the liver, spleen, kidney, heart, and lung, and represented as a

percentage of injected dose per gram of tissue (Figure 3.10). The proportion of injected radiolabel that was measured in the blood, kidney, heart, and lung was between 1.2 and 3.6%, with a significant proportion of the LNP accumulating in the liver and spleen (14 and 11%, respectively). Due to the fenestrated endothelium and microcirculation characteristics, the liver and spleen are expected to be significantly exposed to lipid nanoparticle carriers of <100 nm, as utilized here. About 4.4% of the injected radiolabel per gram of tissue accumulated at the tumor site, corresponding to roughly 6.1 μg siRNA per gram of tissue. With an average tumor weight of 0.09 grams, roughly 0.5 μg of siRNA total accumulated at tumor sites. These data infer that, despite the relatively high accumulation of radiolabelled system in the liver and spleen, the *in vivo* LNP formulation could potentially deliver an siRNA payload to distal 22Rv1 tumor sites, under the assumption that the radiolabel measured at the tumor site was a component of intact siARv-LNP systems.

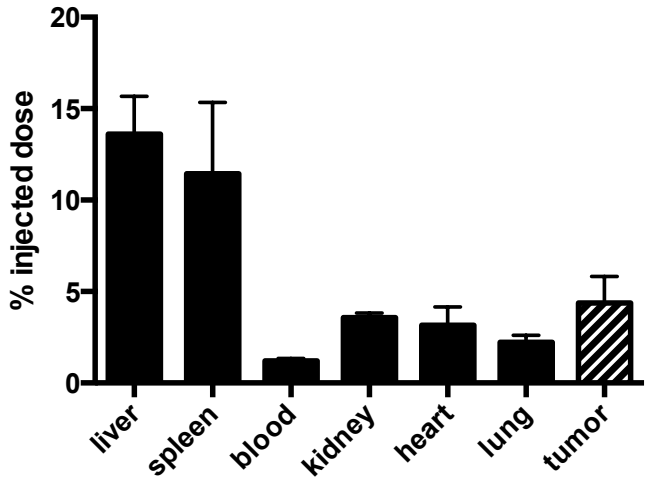

Figure 3.10 Biodistribution of siARv-LNP in mice bearing 22Rv1 xenograft tumors.

Mice were inoculated subcutaneously with 22Rv1 cells in 50% Matrigel. Once tumors reached 250 mm^3, mice were injected with 5 mg/kg siARv-LNP labeled with the lipid tracer [^{14}C]-DSPC. At 24 h post-injection, plasma, tumors, and organs were counted for ^{14}C label using a scintillation counter. The percent recovery in blood was calculated based on a blood volume of 70 ml/kg animal weight. Tumor- and organ-associated radioactivity is expressed as percent injected dose per total organ weight. Data represents mean (± SD); n=8.

3.6 Antitumor efficacy of siARv-LNP in the 22Rv1 xenograft model

After determining the biodistribution properties of the siARv-LNP in mice bearing 22Rv1-derived tumors, the efficacy of the system was tested against siARfl-LNP and siLUC-LNP in the same xenograft model. Twenty days after 22Rv1 cell inoculation, when tumors had reached an average of 100 mm^3, male NRG mice were randomly assigned for treatment with PBS control or 5 mg/kg siARv-LNP, siARfl-LNP, or siLUC-LNP according to the treatment schedule described in Figure 3.11 A. Each treatment group consisted of 11 animals, and a total of 9 intravenous doses were administered to each mouse surviving to the end of the study. One animal from the siARfl-LNP treatment group died prematurely, for reasons unrelated to tumor burden, and was removed from the data analysis. Tumor volume measurements were made three times per week throughout the study, and by day 14 of treatment, siARv-LNP was the only treatment to have significantly maintained a slowed tumor growth relative to the PBS control (Figure 3.11 B). In contrast, siARfl-LNP and siLUC-LNP treatment groups were not able to significantly slow tumor progression compared to the PBS control by the study end.

As shown by the survival curve in Figure 3.11 C, the life span of xenograft-bearing mice treated with siARv-LNP showed improvement over all other treatment groups, with survival defined as the time taken for tumors to reach 1,000 mm^3. The survival rate of the siARv-LNP group was 64% compared to 50% and 46% for that of the siARfl-LNP and siLUC-LNP treatment groups. This corresponds to median survival times of >20 days (undefined by the study parameters), 19.5, and 19 days, respectively. It is important to note that the siARfl- and siLUC-containing LNP had an effect on mouse survival rate, albeit to a lesser degree than siARv-LNP. To address this point, future studies should look at the non-specific effects of the LNP carrier itself, as was exhibited by the *in vitro* MTT studies in 22Rv1 cells. Nonetheless, the

observations on tumor growth and animal survival do indicate that siARv-LNP can exhibit antitumor activity that is superior to that of siARfl-LNP, which targets a smaller AR population, as well as that of a system containing siRNA negative control (siLUC-LNP).

Panel E of Figure 3.11 shows the body weights of mice throughout the 22Rv1 antitumor study. The average body weight of the siARv-LNP-treated mice dropped by 13% after the first three doses, which were administered on consecutive days. However, once the treatments were given less frequently (every three days), the average body weight recovered by day 12 despite the continued repeat dosing. The siARfl-LNP and siLUC-LNP treatment groups did not exhibit similar losses in weight, implying the observed symptoms were siARv-specific and not LNP carrier-specific.

A

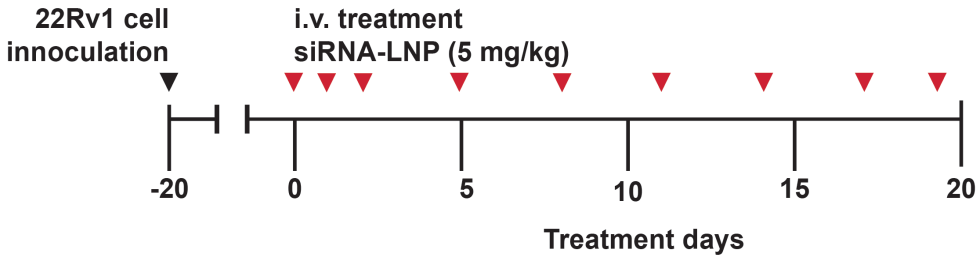
22Rv1 cell
innoculation
i.v. treatment
siRNA-LNP (5 mg/kg)
-20
0
5
10
15
20
Treatment days

B

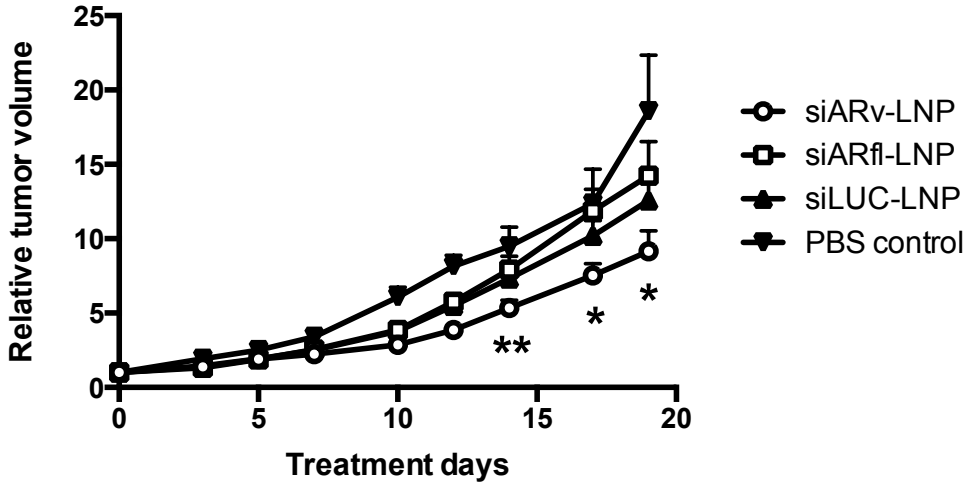
Relative tumor volume
25
20
15
10
5
0
0
5
10
15
20
Treatment days
**
*
*
siARv-LNP
siARfl-LNP
siLUC-LNP
PBS control

C

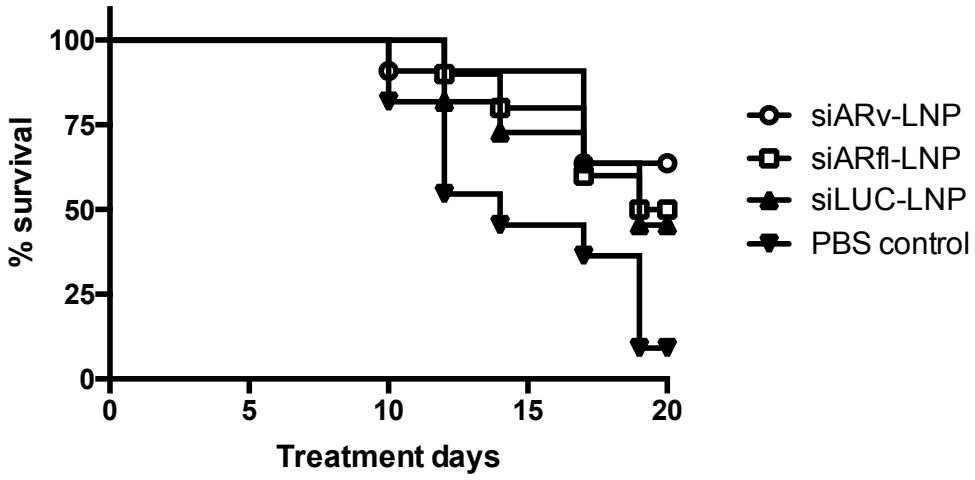
% survival
100
75
50
25
0
0
5
10
15
20
Treatment days
siARv-LNP
siARfl-LNP
siLUC-LNP
PBS control

D

Group	Median survival (days)	P value vs. PBS control
siARv-LNP	>20 or undefined	0.0110
siARfl-LNP	19.5	0.0425
siLUC-LNP	19	0.0533
PBS	14	

E

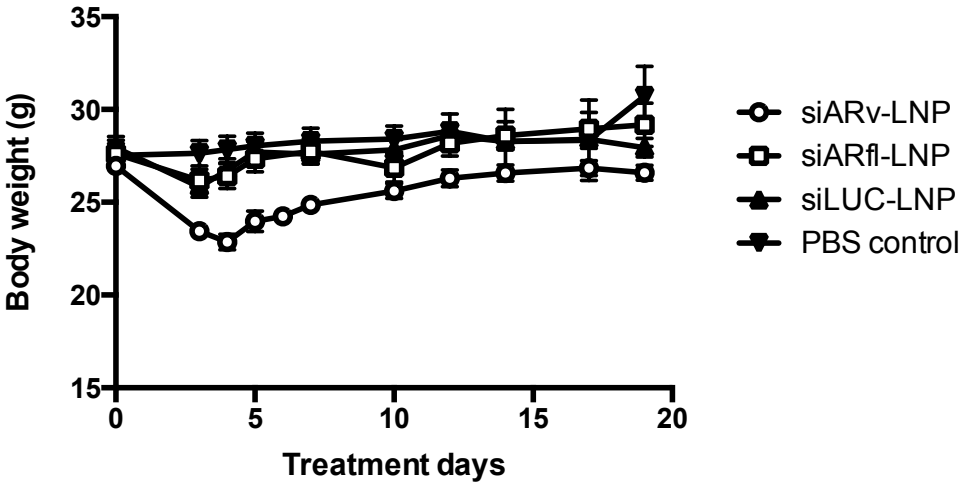

Figure 3.11 Treatment of 22Rv1 xenografts with siARv-LNP slows tumor progression and increases survival rate.

(**A**) Mice were inoculated subcutaneously with 22Rv1 cells. Once tumors reached 100 mm^3, mice were randomly assigned to PBS control or 5 mg siRNA/kg body weight of siARv-LNP, siARfl-LNP, or siLUC-LNP for a total of 9 injections. (**B**) The mean tumor volume relative to treatment day 0 (± SEM), (**C**) survival curves, (**D**) median survival analysis, and (**E**) average body weight (± SEM) were compared between the four groups, with survival defined as the time taken for tumors to reach 1,000 mm^3; **P<0.01 or *P<0.05 siARv-LNP compared with PBS control.

In order to determine whether or not the effects on 22Rv1 tumor volume and animal survival correlated with target gene knockdown, RNA was extracted from tumor tissues of all mice surviving on the final day of the efficacy study, treatment day 20. Only one mouse from the PBS control group survived to the end of the study, therefore mRNA expression levels of each xenograft, and overall target gene knockdown efficiency, was compared to the siLUC-LNP control group using the delta-delta C_T method. Figure 3.12 A-C shows the relative mRNA levels of AR, AR-V7, and PSA of the three treatment groups, respectively. It is clear that by study end, of the three genes tested, AR exhibited the most homogeneous expression within each treatment group (Figure 3.12 A), whereas AR-V7 and PSA xenograft mRNA levels were more heterogeneous (Figure 3.12 B and C, respectively). It is only with the AR gene that the siARv-LNP treatment group exhibited significant knockdown compared to the siLUC-LNP control group. The AR mRNA levels from the siARfl-LNP-treated tumors were not significantly different than those from the siLUC-LNP-treated tumors (Figure 3.12 A). Previous studies performed in collaboration with the Cullis laboratory were able to show >50% target gene knockdown in anti-androgen-resistant, LNCaP-derived xenografts following repeat dosing of siRNA-LNP systems (Yamamoto et al., 2015a). These studies utilized a similar treatment schedule, as well as a similar LNP carrier containing DLin-MC3-DMA ionizable amino lipid and density of 2.5 mol% PEG-DSG lipid coating. The antitumor work presented here could benefit from a future 22Rv1 xenograft study that measures AR, AR-V7, and PSA mRNA and protein levels in tumors following each consecutive dose, in contrast to strictly measuring the respective mRNA levels in tumors at the end of a full treatment schedule. Such a study could better illustrate the efficacy of the siARv-LNP system over time, and better identify limiting factors to tumor gene knockdown, such as tumor size.

A

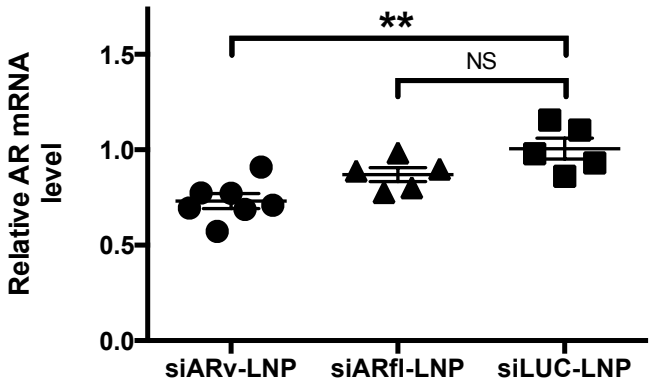
**
NS
Relative AR mRNA level
1.5
1.0
0.5
0.0
siARv-LNP
siARfl-LNP
siLUC-LNP

B

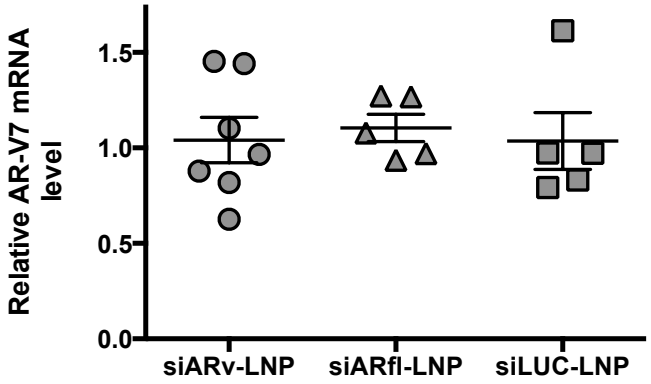
Relative AR-V7 mRNA level
1.5
1.0
0.5
0.0
siARv-LNP
siARfl-LNP
siLUC-LNP

C

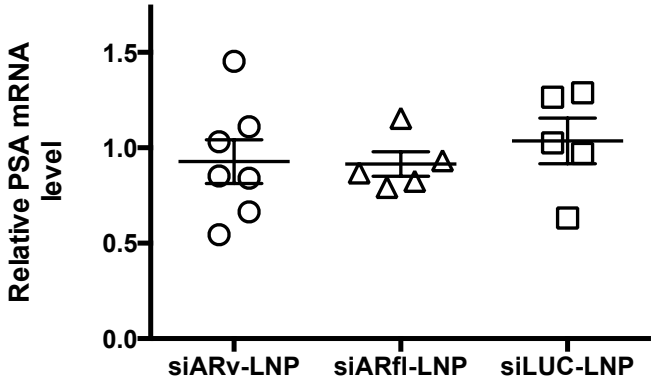
Relative PSA mRNA level
1.5
1.0
0.5
0.0
siARv-LNP
siARfl-LNP
siLUC-LNP

Figure 3.12 Treatment with siARv-LNP results in limited gene knockdown in 22Rv1 xenografts by end of antitumor efficacy study.

RNA was extracted from tumor tissue of all surviving mice at end of study. The (**A**) AR, (**B**) AR-V7, and (**C**) PSA genes were analyzed by qPCR, normalized to the β-actin gene, and expressed as relative mRNA levels to the siLUC-LNP treatment group. Each data point in all three panels represents the gene expression profile of tumor tissue from one animal. Mean values are represented by horizontal bar (± SEM); **P<0.01

Chapter 4: Discussion

The studies outlined in this thesis, which describe the application of an LNP delivery vehicle for siRNA to human prostate cancer and illustrate how this approach functions as a therapeutic in tumor-bearing animals, leave much to be discussed. The following chapter examines the implications of the observations made in this thesis, and their role in elucidating the utilization of such nanoparticle systems for treating distal tumor targets.

4.1 LNP containing siARv for reducing activity of ARs

AR pathway inhibitors like abiraterone acetate and enzalutamide can prolong survival in men with castration-resistant prostate cancer, but resistance to these therapies often develops with reactivation of AR remaining a central driver for this progression (Sharp et al., 2016). The expression of constitutively active AR splice variants is a way in which AR activity continues under these conditions, thus there have been several efforts to target this pathway yielding direct and indirect small-molecule inhibitors of AR NTD function (Antonarakis et al., 2016). However, all of these efforts have yet to make it to the clinical setting. Many of these inhibitors are identified through small-molecule screening efforts, whereby effective compounds are identified from libraries of molecules. In contrast to this approach, siRNA can be specifically designed against a target of choice and, with the appropriate delivery vehicle, can be applied systemically as a genetic drug. Here, multiple siRNA molecules were designed against exon 1 of the AR mRNA (Figure 3.3), which is present in all AR splice variant mRNA. The siARv molecule gave rise to the greatest level of gene silencing in the 22Rv1 model, a result that was mirrored in the reduction of protein levels of ARs (Figure 3.4). To put the scope of this siRNA

screen into perspective, certain screening efforts have utilized over 400 sequences and a four-stage *in vitro* screening process to identify candidate therapeutic siRNAs (Dudek et al., 2014). Although the smaller scale screen described in this thesis was able to identify a potent siRNA molecule, a larger scale screen would provide a library of functional target-specific sequences should alternate molecules need to be utilized at later stages of the siRNA developmental process. An example of such a case appeared in this investigation, when it became apparent that siARv induces some *in vivo* toxicity in mice (Figure 3.11). Additional aspects of screening siRNA molecules include dose titrations and analysis of the duration of gene knockdown to further characterize overall functionality (Dudek et al., 2014). The relative persistence of siARv-mediated knockdown *in vitro* was only analyzed for up to 48 hours; however, siARv and its 2'-O-methylated product silenced AR mRNAs in the 22Rv1 model to a degree where very little detectable protein product was visible by western blot (Figure 3.4). Ultimately, the modified siARv molecule was carried forward to more downstream functional assays.

As the ultimate goal was to deliver siRNA by use of the LNP system, siARv was encapsulated into DLin-MC3-DMA-containing nanoparticles and *in vitro* functional experiments were carried out in 22Rv1 and LNCaP human prostate cancer cells. The LNP systems utilized for the studies described in this thesis were mainly prepared by use of a T-junction mixer (Kulkarni et al., 2018), which facilitates rapid mixing of the lipid and siRNA components, and formation of monodisperse particles (Figure 3.5). These biocompatible siRNA delivery vehicles serve as a means to deliver the payload to the cytosol of the cell, facilitating cell uptake and endosomal escape (Cullis & Hope, 2017). These systems also show rapid and effective uptake into human-derived cancer cells in culture (Lee et al., 2012; Tam et al., 2012). As expected on the basis of siARv activity and DLin-MC3-DMA-LNP potency, siARv-LNP systems exhibited

potent knockdown of ARs in 22Rv1 and LNCaP cell lines (Figure 3.6). The LNP achieved ~80% knockdown of both full-length AR and AR-V7 mRNA, at concentrations below those utilized with the Lipofetamine RNAiMAX-mediated transfection (Figure 3.3). The siARv-LNP was clearly equipotent against AR genes in both the 22Rv1 and LNCaP human prostate cancer cell lines, and the knockdown of AR and AR-V7 mRNA was comparable to that seen with siRNA targeting the clusterin gene in LNCaP-derived cells utilizing similar LNP systems (Yamamoto et al., 2015a). Treatment with the siARv-LNP system also resulted in the reduction of PSA mRNA levels, a functional indicator of the knockdown of ARs (Figure 3.5). With LNCaP cells having extremely low AR-V7 levels, and expressing no detectable levels of the AR-V7 protein, it was to be expected that the siARv-LNP system would not be beneficial over the siARfl-LNP in terms of affecting levels of PSA mRNA. However, as the siARv-LNP system is efficient in both 22Rv1 and LNCaP cell lines, this highlights the broader application of the AR mRNA exon 1-targeted system over that of the siARfl-LNP. Taken together, these results describe the identification of the siARv from a panel of siRNA targeting exon 1 of AR mRNA, confirm the utility of the DLin-MC3-DMA-LNP carrier for transfection of siRNA to human prostate cancer cells *in vitro*, and illustrate that this delivery confers silencing of target genes, as well as their downstream transcriptional targets, in both 22Rv1 and LNCaP models. Essentially, the siARv-LNP system shares its downstream target with an AR NTD inhibitor, and the siARfl-LNP with that of a general anti-androgen, but both in the form of genetic drug carrier systems.

4.2 Effect of the siARv-LNP system on cell viability

Previous work comparing the effects on cell viability of ASOs targeting exon 1 and exon 8 of AR mRNA showed a significant reduction in 22Rv1 cell viability for exon 1-targeted ASO

over that targeting exon 8 (Yamamoto et al., 2015b). In addition, siRNA-mediated knockdown of AR-V7 mRNA indicated that the biologic significance of AR splice variants is cell-type-specific. It was shown that 22Rv1 cell growth is driven by variant ARs, while full-length AR predominantly drives the growth of an enzalutamide-resistant LNCaP cell line despite these cells expressing AR-V7 protein. Knockdown of variant AR mRNA was also shown to induce apoptosis in the 22Rv1 model, specifically (Yamamoto et al., 2015b). The effects on cell viability of the siARv-LNP and siARfl-LNP systems were compared in the 22Rv1 and LNCaP cell lines, models with differing AR molecular phenotypes, and the results agreed with previous findings. Again, these findings highlighted the broader applicability of the siARv-LNP system, as it was able to significantly reduce the cell viability of both 22Rv1 and LNCaP at all concentrations tested compared to the siLUC-LNP control formulation (Figure 3.8). Also noted by the *in vitro* cell viability experiments, the 22Rv1 cell line was specifically susceptible to toxicity from the control formulation, in comparison to the LNCaP and PC3 models. This reduction in viability of 22Rv1 cells *in vitro* mediated by the control formulation was also demonstrated in early effects on relative xenograft volume *in vivo* (Figure 3.11). Future studies should investigate the cause of the non-specific siRNA-LNP-based reduction of 22Rv1 cell viability, and whether it is correlated to the exogenous oligonucleotide payload or the lipid delivered to the cells. Ultimately, these findings suggest that certain cell culture model systems have a heightened sensitivity to the DLin-MC3-DMA-containing siRNA-LNP system over others.

4.3 Potency of the siARv-LNP system at distal tumor sites

Due to the enhanced permeability and retention (EPR) effect, LNP can theoretically accumulate at solid tumor sites by transport from systemic circulation. There are, however, factors that can impact the efficacy of this passive delivery of LNP, such as tumor size, vascularization of the tumor tissue, as well as the tumor microenvironment (Allen & Cullis, 2013). The biodistribution of siRNA-LNP systems has been extensively studied, showing considerable accumulation at the liver (Mui et al., 2013; Chen et al., 2016), but has yet to be measured in tumor-bearing mice and at doses as high as 5 mg siRNA/kg animal weight. The efforts employed here to increase circulation lifetime and maximize the accumulation of LNP to 22Rv1 xenografts involved three facets of the nanoparticle system. Firstly, PEG-DSG was incorporated into the LNP system, a lipid-conjugated polymer that coats the particle and exhibits slowed desorption both *in vitro* and *in vivo* (Mui et al., 2013; Chen et al., 2016). Secondly, an optimal PEG-lipid molar content was employed, based on the previous studies showing improved tumor gene knockdown efficacy of 2.5 mole % PEG-DSG over systems containing 5 mole % PEG-DSG (Yamamoto et al., 2015a). Lastly, the ratio of lipid to siRNA in the system was increased two-fold, as previous studies were able to show that this leads to an increased *in vivo* siRNA-LNP potency for systems of a similar size (Chen et al., 2016). The rationale in increasing the ratio of lipid to siRNA is that this corresponds to a greater amount of nanoparticles per siRNA dose, and in theory should lead to an increased likelihood of siRNA delivery to the cytosol of tumor cells. This is an important factor to investigate, as the main barrier to applying such LNP systems to a xenograft model is the delivery of the carriers to extrahepatic sites. The main question is whether or not the amount of injected dose that reached the 22Rv1 tumors is satisfactory in facilitating target gene knockdown and an ultimate antitumor effect. It was shown

that 5% of the injected dose per gram of tissue accumulated at xenografts, corresponding to roughly 6 μg siRNA/g tissue. In previous studies, the silencing of a luciferase reporter gene was assessed in subcutaneous PC-3-derived tumors utilizing DLin-KC2-DMA-containing LNP systems with 2.5 mole % PEG-DSG (Yamamoto et al., 2015a). These LNP containing luciferase-targeted siRNA decreased luciferase expression to 75% in the subcutaneous xenografts following 5 consecutive daily intravenous doses compared to a control formulation (Yamamoto et al., 2015a). This shows that consecutive daily doses, utilizing a system that is less potent than DLin-MC3-DMA-containing LNP, can lead to effective knockdown at distal tumor sites, and that perhaps the consecutive dosing early in tumor development plays a role in delivery of enough siRNA for substantive target gene knockdown. These consecutive system administration results were taken into consideration when planning the dosing schedule for the 22Rv1 antitumor study.

With repeat doses of 5 mg siRNA/kg animal weight, LNP containing siARv exhibited improved antitumor activity over those targeting full-length AR mRNA (siARfl-LNP) or those containing a negative control siRNA (siLUC-LNP), by study end. These results were also reflected in the relative survival of the treatment groups (Figure 3.11). The *in vivo* results were consistent with the *in vitro* findings of siARv-LNP having a greater impact on cell viability than systems containing siARfl or siLUC; however, both siARfl and siLUC appear to slow 22Rv1 tumor growth more effectively than the PBS control at certain points of the treatment schedule, particularly between days 7 and 12. The results also indicate that target gene knockdown is limited with repeat intravenous injections of the DLin-MC3-DMA-LNP siARv formulation by study end (Figure 3.12). These results are inconsistent with previous studies using LNCaP-derived xenografts and LNP delivering full-length AR mRNA-targeted siRNA, which showed

considerable knockdown of AR in tumors, decreased serum PSA levels, but no significant effect on tumor volume (Lee et al., 2012; Lee et al., 2016). For the *in vivo* studies outlined in this thesis, an increased lipid-to-siRNA ratio was utilized in order to promote delivery of more nanoparticles to the disease site, and thus increase the chance for siRNA transfection into tumor cells. Comparing the knockdown efficacies of this system to previous studies utilizing the DLin-MC3-DMA-LNP system and a similar dosing schedule (Yamamoto et al., 2015a), there is no obvious improvement in potency. While it is difficult to make direct comparisons between the two studies, as they utilize different prostate cancer xenograft models, dissimilar siRNA design, as well as different target genes, there is no strong evidence that increasing the lipid-to-siRNA ratio of LNP improves the potency at distal tumor sites, as it does the potency of systems in hepatocytes (Chen et al., 2016). Additionally, in terms of siRNA delivery, the amount of formulation that can penetrate into tumor tissue could also be limited. After LNP passively accumulate at solid tumors, there are a number of anatomical and physiological barriers that need to be overcome before uptake into target cells can occur. The abnormal tumor vasculature, as well as the network of extracellular matrix, promotes the non-homogeneous distribution of the drug payload at tumor sites (Jain & Stylianopoulos, 2010). A substantial increase in the potency of *in vivo* siARv-LNP delivery systems may be required to achieve a comparable impact on both tumor volume and gene knockdown by study end. In my opinion, one of the most pressing future experiments to perform is to determine the knockdown efficacy of the siARv-LNP system starting in tumors of lower volumes, ~100 mm^3. The levels of target mRNAs and protein should be more thoroughly assessed overtime, as tumor size grows, instead of at study end alone when tumor size could be limiting the effectiveness of LNP delivery of siRNA to tumor cells. It is important to note that previous studies utilizing *in vitro*-optimized siRNAs, delivered by lipid

nanoparticle formulations to orthotopic liver tumors in mice resulted in significant target gene knockdown (Dudek et al., 2014), and that the main limitation to siARv-LNP efficacy in the animal model likely lies in the delivery of the vehicle to the disease site, a limitation that is possibly exacerbated by increasing tumor volume, and not the potency of the siARv molecule in tumor cells.

While the ability of the siARv-LNP system to significantly slow 22Rv1-derived tumor progression and enhance animal survival relative to a PBS control group was demonstrated, the apparent *in vivo* toxicity of this molecule demands further discussion. Following the first three consecutive doses of the 22Rv1 antitumor study, there was a significant reduction in body weight for the siARv-LNP treatment group alone (Figure 3.11 E). As the groups receiving injections of siARfl-LNP or siLUC-LNP did not exhibit comparable losses in body weight, it is implied that the off-target effects exhibited in mice were siARv-specific, and not a result of the LNP carrier itself. An obvious factor that differentiates the siARv molecule from the siARfl and siLUC sequences is that siARv is a Dicer-substrate siRNA molecule, whereas siARfl and siLUC are standard siRNAs. Due to the fact that Dicer-substrate siRNAs are processed to predictable 21-nucleotides sequences, the number of off-target effects is not expected to be substantially different than those resulting from standard siRNAs (Amarzguioui et al., 2006). Another differentiating factor of the siARv molecule is an alternative modification pattern to that of siARfl and siLUC; however, modification with 2'-O-Me chemistry is generally well tolerated (Robbins et al., 2009; Jackson & Linsley, 2010), and does not provide a rationale for the side effects exhibited in the severely immunodeficient NRG mice. Although there was marked weight gain after the first three siARv-LNP injections, when dosing was limited to two injections

per week, the extent to which animals lost weight was close to humane endpoint and thus should be remedied by future studies.

Overall, due to the persistent role that ARs play in the development of castration-resistant prostate cancer, there is considerable clinical interest in reducing the activity of ARs in this late-stage disease. The work described in this thesis investigates an alternative approach to targeting the AR signaling pathway, by use of oligonucleotide-mediated gene knockdown, in contrast to the small-molecule approaches that directly or indirectly target the AR protein, or the production of AR-activating androgens. The results indicate that DLin-MC3-DMA-containing siARv-LNP demonstrate modest anticancer activity *in vivo* by significantly slowing 22Rv1 tumor growth. As both siRNA and LNP technology advance, improvements in potency and specificity of a prostate cancer-targeted system seem within reason.

Chapter 5: Conclusions and Future Directions

5.1 Concluding remarks

The work presented in this thesis explores the utility of the DLin-MC3-DMA-LNP system for delivery of siRNA targeting full-length and variant ARs as a treatment for advanced stages of prostate cancer. Potential issues remain to be addressed to warrant further development of the siARv-LNP system for such an application. These points include the non-specific effects of the LNP carrier itself, particularly on 22Rv1 growth, as well as further optimization of the siARv molecule to mitigate the observed *in vivo* toxic side effects. As the potency of the siARv-LNP remains to be improved upon, future work may focus on incorporation of small-molecule prodrugs into the LNP system that could either enhance delivery of the siRNA payload to the cytosol or provide additive anticancer effects.

5.2 Deciphering the 22Rv1 susceptibility to control LNP

While it was shown that treatment of 22Rv1 cells with siARv-LNP resulted in marked reduction in cell viability compared to that of siARfl-LNP, providing support for the approach of treating AR variant-dependent prostate cancer with siARv, it remains to be determined why this prostate cancer model has particular susceptibility to the siLUC-LNP formulation. At the siRNA concentrations tested *in vitro*, both the LNCaP and PC3 human prostate cancer cell lines did not exhibit a similar sensitivity to the control system. This particular off-target effect also appears to lead to some limited *in vivo* efficacy of formulations containing the negative control siRNA. As the previous studies that utilized these LNP systems for treatment of LNCaP-derived xenografts did not report similar effects of control carriers on cell health or tumor volume (Lee et al., 2012;

Yamamoto et al., 2015a; Lee et al., 2016), the cause of such 22Rv1 susceptibility, whether it be the siRNA payload or the lipid components of the nanoparticle system, remains to be deciphered. Certain siRNA delivery materials can induce gene expression changes, which can potentially cause toxicity and other off-target effects. Commonly used transfection reagents, lipofectin and oligofectamine, have been shown to induce their own gene expression signatures even in the absence of siRNA in certain human cell lines, affecting genes known to be involved in cell proliferation, differentiation, and apoptosis (Omidi et al., 2003). In addition, it was demonstrated that the gene signature of a polypropylenimine-based delivery system can be markedly different between cell lines (Omidi et al., 2005). While delivery materials alone can induce gene expression changes and cause toxicity, the induced off-target effects should be taken into consideration in gene therapy as they may interfere with the desired genotypic and phenotypic end-points. The importance of further investigating the cause of 22Rv1 susceptibility to siRNA-LNP lies in the reduction of off-target effects and the development of a more specific genetic drug.

5.3 Addressing the *in vivo* toxicity of the siARv molecule

The 22Rv1 antitumor studies were carried out in NRG mice, extremely immunodeficient animals with mutations that result in B cell, T cell, and NK cell deficiency (Pearson et al., 2008). The activation of an innate immune response to the siARv molecule, which has been shown to occur following administration of certain exogenous siRNAs (Robbins et al., 2009), would not be a viable explanation to the side effects that occurred in these animals. The knockdown of any endogenous gene could lead to unanticipated direct toxicity, including that mediated by siARv; however, the EPI-506 drug showed a favorable safety profile during clinical testing (Chi et al.,

2017) and does not indicate that AR NTD-targeted therapies confer toxic side effects. Nonetheless, in the case of the antitumor study in NRG mice, the siARv molecule is directed to the human AR gene (NM_000044) and there is no significant sequence similarity between siARv and the mouse AR gene (NM_013476), negating any likelihood that the exhibited *in vivo* toxicity is an on-target effect. Alternatively, the biodistribution study for siARv-LNP indicated that a significant proportion of injected nanoparticles are delivered to the liver. Studies utilizing liver-targeted siRNAs at toxicological doses in rodents demonstrated that alterations in the chemistry of these siRNAs, or perturbation of the RNAi pathway, had no effect on the degree of hepatotoxicity (Janas et al., 2018). Instead, they showed that seed hybridization-based off-target effects were the major driver of hepatotoxicity, implicating sequence-specific RNAi-based off-target effects as the major driver of hepatotoxicity. Such off-target events could be the cause of the side effects exhibited in NRG mice after consecutive doses of LNP-encapsulated siARv. These unexpected results highlight the importance of screening siRNA sequences *in vivo*, in addition to a panel of target diseased cells *in vitro*, prior to carrying out antitumor efficacy studies. Although design tools can help in deciding among sequences on the basis of the number of potential off-targets, there is no reliable substitute for experimental determination of siRNA specificity (Amarzguioui et al., 2006). To better assess the effect of siARv on animal health, a study screening for liver toxicity upon repeat dosing of siARv-LNP should be carried out, analyzing serum liver transaminases and liver histopathology. Additional AR mRNA exon 1-targeted siRNA sequences could be analyzed for *in vivo* toxic side effects, and a potentially equipotent, but less toxic molecule, could be identified.

5.4 Improving the *in vivo* activity of siARv-LNP

The doses utilized in the 22Rv1 antitumor study, in conjunction with the modest anticancer potency, limit the siARv-LNP system from consideration as a viable nucleic acid-based treatment of prostate cancer. Two potential ways in which the activity of siARv-LNP at distal tumor sites could be improved upon include enhancing the delivery of the carriers to the tumor site, or designing the LNP systems to be more potent upon reaching the delivery site.

5.4.1 Delivery of siARv to tumor cells

With regard to more effective delivery of siARv to tumor tissue, two approaches have already been examined. The first involves using a PEG lipid that has a slowed desorption rate from the LNP (PEG-DSG) and thus an increased circulation lifetime, resulting in greater accumulation at tumor sites. The second involves increasing the molar content of the PEG lipid in the LNP formulation (Lee et al., 2016). Unfortunately, a high density (5 mol%) of LNP-coating PEG-DSG lipid results in a reduction in potency at distal tumor sites (Yamamoto et al., 2015a). This can be attributed to the PEG lipid interfering with intracellular uptake of particles, or interfering with release of siRNA to the cytosol (Gilleron et al., 2013). This can be rectified to some extent by incorporating PEG lipid modified with targeting ligands, such as a ligand targeting PSMA (Tam et al., 2012; Lee et al., 2016); however, the gains are relatively minor and there is no strong evidence for improvement over non-targeted systems with a lower density (2.5 mol%) of PEG-DSG. Future studies could investigate the combination of the PSMA-targeted PEG lipid with an LNP system containing a total of 2.5 mol% PEG-DSG. This is an approach that has yet to be investigated, and could result in improved efficacy of the systems utilized in the 22Rv1 antitumor study.

5.4.2 Modifying the siARv design

This leaves the need to increase the potency of the siARV-LNP system itself upon reaching the tumor cell. In line with optimizing an siARv molecule for reduced toxic side effects, the design can also be altered for improved and prolonged knockdown of the target genes. In terms of clinical development of siRNA-based therapies, there are several generations of modification motifs proven to enhance oligonucleotide knockdown potency (Huang, 2017). For the work presented in this thesis, a single siRNA modification pattern was tested in 22Rv1 cells *in vitro* and was carried forward to all subsequent studies, leaving room to improve the *in vivo* oligonucleotide potency based on a sequence modification approach. In addition, only a single AR variant-targeted siRNA molecule was tested *in vivo*, and without a thorough investigation of the duration of AR knockdown. As mentioned above, experiments can be performed to investigate the means by which an siRNA sequence can exhibit improved and prolonged knockdown capabilities.

5.4.3 Small-molecule and siARv-LNP combination approaches

Lastly, it has been noted that the efficiency of current gold standard siRNA-LNP systems for intracellular delivery of the siRNA payload is only 1-2% (Gilleron et al., 2013; Sahay et al., 2013). This is due to siRNA entrapment within endosomes or recycling of siRNA back to the extracellular space, creating another challenge for lipid carrier technology: achieving more efficient delivery beyond the endosomal compartments of target cells. Approaches that enhance endosomal escape and cytosolic delivery of the LNP siRNA cargo, such as the application of small-molecule antagonists to vesicular trafficking, could potentially rectify this problem. A

previous study has shown that cotreatment with an inhibitor of Niemann-Pick type C1 (NPC1), a late endosomal/lysosomal membrane protein required for efficient extracellular recycling of endosomal contents, resulted in a four-fold increase in the gene-silencing potency of siRNA-LNP (Wang et al., 2016). The Cullis laboratory has described the design parameters for prodrug derivatives of dexamethasone, an immunosuppressive agent, containing degradable ester linkages and a degree of hydrophobicity that promotes prodrug incorporation into LNP during the formulation process (Chen et al., 2018). Inclusion of a hydrophobic prodrug version of the NPC1 inhibitor in the lipid formulation may prove useful for increasing gene-silencing potency of the siARv-LNP system. Another way in which the effectiveness of the siARv-LNP system, specifically, could be improved is by way of a chemotherapeutic combination approach. Previous efforts have shown that targeting the NTD of AR with an earlier derivative of EPI-506 enhances the antitumor effect of docetaxel in the 22Rv1 model (Martin et al., 2014). Using a similar prodrug strategy as described above, chemotherapeutic agents could be incorporated into the LNP formulation to afford a small-molecule and siRNA combination approach. Incorporation of a lipophilic prodrug of docetaxel into the siARv-LNP system during the formulation process could provide a means to potentially improve upon the modest *in vivo* anticancer efficacy of solely silencing AR gene expression, and is an investigation that is currently being undertaken by the Cullis laboratory.

References

Adams, D., Gonzalez-Duarte, A., O'Riordan, W. D., Yang, C.-C., Ueda, M., Kristen, A. V., Tournev, I., Schmidt, H. H., Coelho, T., Berk, J. L., et al. (2018). Patisiran, an RNAi Therapeutic, for Hereditary Transthyretin Amyloidosis. *New England Journal of Medicine, 379*(1), 11-21.

Ahmann, F. R., Citrin, D. L., deHaan, H. A., Guinan, P., Jordan, V. C., Kreis, W., Scott, M., & Trump, D. L. (1987). Zoladex: a sustained-release, monthly luteinizing hormone-releasing hormone analogue for the treatment of advanced prostate cancer. *Journal of Clinical Oncology, 5*(6), 912-917.

Akinc, A., Querbes, W., De, S., Qin, J., Frank-Kamenetsky, M., Jayaprakash, K. N., Jayaraman, M., Rajeev, K. G., Cantley, W. L., Dorkin, J. R., et al. (2010). Targeted delivery of RNAi therapeutics with endogenous and exogenous ligand-based mechanisms. *Molecular Therapy, 18*(7), 1357-1364.

Akinc, A., Zumbuehl, A., Goldberg, M., Leshchiner, E. S., Busini, V., Hossain, N., Bacallado, S. A., Nguyen, D. N., Fuller, J., Alvarez, R., et al. (2008). A combinatorial library of lipid-like materials for delivery of RNAi therapeutics. *Nature Biotechnology, 26*(5), 561-569.

Allen, T. M. (1994). The use of glycolipids and hydrophilic polymers in avoiding rapid uptake of liposomes by the mononuclear phagocyte system. *Advanced Drug Delivery Reviews, 13*(3), 285-309.

Allen, T. M., & Cullis, P. R. (2013). Liposomal drug delivery systems: from concept to clinical applications. *Advanced Drug Delivery Reviews, 65*(1), 36-48.

Amarzguioui, M., Lundberg, P., Cantin, E., Hagstrom, J., Behlke, M. A., & Rossi, J. J. (2006). Rational design and in vitro and in vivo delivery of Dicer substrate siRNA. *Nature Protocols, 1*, 508.

Andersen, R. J., Mawji, N. R., Wang, J., Wang, G., Haile, S., Myung, J.-K., Watt, K., Tam, T., Yang, Y. C., Bañuelos, C. A., et al. (2010). Regression of Castrate-Recurrent Prostate Cancer by a Small-Molecule Inhibitor of the Amino-Terminus Domain of the Androgen Receptor. *Cancer Cell, 17*(6), 535-546.

Antonarakis, E. S., Chandhasin, C., Osbourne, E., Luo, J., Sadar, M. D., & Perabo, F. (2016). Targeting the N-Terminal Domain of the Androgen Receptor: A New Approach for the Treatment of Advanced Prostate Cancer. *Oncologist, 21*(12), 1427-1435.

Antonarakis, E. S., Lu, C., Wang, H., Luber, B., Nakazawa, M., Roeser, J. C., Chen, Y., Mohammad, T. A., Chen, Y., Fedor, H. L., et al. (2014). AR-V7 and resistance to enzalutamide and abiraterone in prostate cancer. *New England Journal of Medicine, 371*(11), 1028-1038.

Asangani, I. A., Dommeti, V. L., Wang, X., Malik, R., Cieslik, M., Yang, R., Escara-Wilke, J., Wilder-Romans, K., Dhanireddy, S., Engelke, C., et al. (2014). Therapeutic targeting of BET bromodomain proteins in castration-resistant prostate cancer. *Nature, 510*(7504), 278-282.

Attard, G., Belldegrun, A. S., & de Bono, J. S. (2005). Selective blockade of androgenic steroid synthesis by novel lyase inhibitors as a therapeutic strategy for treating metastatic prostate cancer. *BJU International, 96*(9), 1241-1246.

Bagshaw, M. A., Kaplan, H. S., & Sagerman, R. H. (1965). Linear Accelerator Supervoltage Radiotherapy. *Radiology, 85*, 121-129.

Bangham, A. D., & Horne, R. W. (1964). Negative staining of phospholipids and their structural modification by surface-active agents as observed in the electron microscope. *Journal of Molecular Biology, 8*(5), 660-668.

Behlke, M. A. (2008). Chemical Modification of siRNAs for In Vivo Use. *Oligonucleotides, 18*(4), 305-320.

Belliveau, N. M., Huft, J., Lin, P. J., Chen, S., Leung, A. K., Leaver, T. J., Wild, A. W., Lee, J. B., Taylor, R. J., Tam, Y. K., et al. (2012). Microfluidic Synthesis of Highly Potent Limit-size Lipid Nanoparticles for In Vivo Delivery of siRNA. *Molecular Therapy. Nucleic Acids, 1*(8), e37.

Beltran, H., Yelensky, R., Frampton, G. M., Park, K., Downing, S. R., MacDonald, T. Y., Jarosz, M., Lipson, D., Tagawa, S. T., Nanus, D. M., et al. (2013). Targeted next-generation sequencing of advanced prostate cancer identifies potential therapeutic targets and disease heterogeneity. *European Urology, 63*(5), 920-926.

Berthold, D. R., Pond, G. R., Soban, F., de Wit, R., Eisenberger, M., & Tannock, I. F. (2008). Docetaxel plus prednisone or mitoxantrone plus prednisone for advanced prostate cancer: updated survival in the TAX 327 study. *Journal of Clinical Oncology, 26*(2), 242-245.

Callewaert, L., Van Tilborgh, N., & Claessens, F. (2006). Interplay between two hormone-independent activation domains in the androgen receptor. *Cancer Research, 66*(1), 543-553.

Cao, B., Qi, Y., Zhang, G., Xu, D., Zhan, Y., Alvarez, X., Guo, Z., Fu, X., Plymate, S. R., Sartor, O., et al. (2014). Androgen receptor splice variants activating the full-length receptor in mediating resistance to androgen-directed therapy. *Oncotarget, 5*(6), 1646-1656.

Chan, S. C., Selth, L. A., Li, Y., Nyquist, M. D., Miao, L., Bradner, J. E., Raj, G. V., Tilley, W. D., & Dehm, S. M. (2015). Targeting chromatin binding regulation of constitutively active AR variants to overcome prostate cancer resistance to endocrine-based therapies. *Nucleic Acids Research, 43*(12), 5880-5897.

Chen, S., Tam, Y. Y. C., Lin, P. J. C., Sung, M. M. H., Tam, Y. K., & Cullis, P. R. (2016). Influence of particle size on the in vivo potency of lipid nanoparticle formulations of siRNA. *Journal of Controlled Release, 235*, 236-244.

Chen, S., Zaifman, J., Kulkarni, J. A., Zhigaltsev, I. V., Tam, Y. K., Ciufolini, M. A., Tam, Y. Y. C., & Cullis, P. R. (2018). Dexamethasone prodrugs as potent suppressors of the immunostimulatory effects of lipid nanoparticle formulations of nucleic acids. *Journal of Controlled Release, 286*, 46-54.

Chi, K. N., Vaishampayan, U. N., Gordon, M. S., Smith, D. C., Rudsinski, E., De Haas-Amatsaleh, A., Thapar, N., Perabo, F., & Montgomery, R. B. (2017). Efficacy, safety, tolerability, and pharmacokinetics of EPI-506 (ralaniten acetate), a novel androgen receptor (AR) N-terminal domain (NTD) inhibitor, in men with metastatic castration-resistant prostate cancer (mCRPC) progressing after enzalutamide and/or abiraterone. *Journal of Clinical Oncology, 35*, 5032-5032.

Cleutjens, K. B., van Eekelen, C. C., van der Korput, H. A., Brinkmann, A. O., & Trapman, J. (1996). Two androgen response regions cooperate in steroid hormone regulated activity of the prostate-specific antigen promoter. *Journal of Biological Chemistry, 271*(11), 6379-6388.

Cooke, B. A., & Sullivan, M. H. (1985). The mechanisms of LHRH agonist action in gonadal tissues. *Molecular and Cellular Endocrinology, 41*(2-3), 115-122.

Cornford, P., Bellmunt, J., Bolla, M., Briers, E., De Santis, M., Gross, T., Henry, A. M., Joniau, S., Lam, T. B., Mason, M. D., et al. (2017). EAU-ESTRO-SIOG Guidelines on Prostate Cancer. Part II: Treatment of Relapsing, Metastatic, and Castration-Resistant Prostate Cancer. *European Urology, 71*(4), 630-642.

Crawford, E. D., & Hou, A. H. (2009). The role of LHRH antagonists in the treatment of prostate cancer. *Oncology (Williston Park), 23*(7), 626-630.

Cullis, P. R., & Hope, M. J. (2017). Lipid Nanoparticle Systems for Enabling Gene Therapies. *Molecular Therapy, 25*(7), 1467-1475.

D'Amico, A. V., Whittington, R., Malkowicz, S. B., Schultz, D., Blank, K., Broderick, G. A., Tomaszewski, J. E., Renshaw, A. A., Kaplan, I., Beard, C. J., et al. (1998). Biochemical outcome after radical prostatectomy, external beam radiation therapy, or interstitial radiation therapy for clinically localized prostate cancer. *JAMA, 280*(11), 969-974.

de Bono, J. S., Oudard, S., Ozguroglu, M., Hansen, S., Machiels, J. P., Kocak, I., Gravis, G., Bodrogi, I., Mackenzie, M. J., Shen, L., et al. (2010). Prednisone plus cabazitaxel or mitoxantrone for metastatic castration-resistant prostate cancer progressing after docetaxel treatment: a randomised open-label trial. *Lancet, 376*(9747), 1147-1154.

Dudek, H., Wong, D. H., Arvan, R., Shah, A., Wortham, K., Ying, B., Diwanji, R., Zhou, W., Holmes, B., Yang, H., et al. (2014). Knockdown of β-catenin with Dicer-Substrate siRNAs Reduces Liver Tumor Burden In vivo. *Molecular Therapy, 22*(1), 92-101.

Eisermann, K., Wang, D., Jing, Y., Pascal, L. E., & Wang, Z. (2013). Androgen receptor gene mutation, rearrangement, polymorphism. *Translational Andrology and Urology, 2*(3), 137-147.

Elbashir, S. M., Harborth, J., Lendeckel, W., Yalcin, A., Weber, K., & Tuschl, T. (2001). Duplexes of 21-nucleotide RNAs mediate RNA interference in cultured mammalian cells. *Nature, 411*(6836), 494-498.

Fang, Y., Fliss, A. E., Robins, D. M., & Caplan, A. J. (1996). Hsp90 regulates androgen receptor hormone binding affinity in vivo. *Journal of Biological Chemistry, 271*(45), 28697-28702.

Felgner, J. H., Kumar, R., Sridhar, C. N., Wheeler, C. J., Tsai, Y. J., Border, R., Ramsey, P., Martin, M., & Felgner, P. L. (1994). Enhanced gene delivery and mechanism studies with a novel series of cationic lipid formulations. *Journal of Biological Chemistry, 269*(4), 2550-2561.

Ferraldeschi, R., Welti, J., Powers, M. V., Yuan, W., Smyth, T., Seed, G., Riisnaes, R., Hedayat, S., Wang, H., Crespo, M., et al. (2016). Second-Generation HSP90 Inhibitor Onalespib Blocks mRNA Splicing of Androgen Receptor Variant 7 in Prostate Cancer Cells. *Cancer Research, 76*(9), 2731.

Fire, A., Xu, S., Montgomery, M. K., Kostas, S. A., Driver, S. E., & Mello, C. C. (1998). Potent and specific genetic interference by double-stranded RNA in Caenorhabditis elegans. *Nature, 391*(6669), 806-811.

Gantier, M. P., & Williams, B. R. (2007). The response of mammalian cells to double-stranded RNA. *Cytokine Growth Factor Reviews, 18*(5-6), 363-371.

Gilleron, J., Querbes, W., Zeigerer, A., Borodovsky, A., Marsico, G., Schubert, U., Manygoats, K., Seifert, S., Andree, C., Stoter, M., et al. (2013). Image-based analysis of lipid nanoparticle-mediated siRNA delivery, intracellular trafficking and endosomal escape. *Nature Biotechnology, 31*(7), 638-646.

Gregoriadis, G. (1973). Drug entrapment in liposomes. *FEBS Letters, 36*(3), 292-296.

Gregoriadis, G., & Ryman, B. E. (1971). Liposomes as carriers of enzymes or drugs: a new approach to the treatment of storage diseases. *Biochemical Journal, 124*(5), 58P.

Grino, P. B., Griffin, J. E., & Wilson, J. D. (1990). Testosterone at high concentrations interacts with the human androgen receptor similarly to dihydrotestosterone. *Endocrinology, 126*(2), 1165-1172.

Guo, Z., Yang, X., Sun, F., Jiang, R., Linn, D. E., Chen, H., Chen, H., Kong, X., Melamed, J., Tepper, C. G., et al. (2009). A novel androgen receptor splice variant is up-regulated during prostate cancer progression and promotes androgen depletion-resistant growth. *Cancer Research, 69*(6), 2305-2313.

Hafez, I. M., Maurer, N., & Cullis, P. R. (2001). On the mechanism whereby cationic lipids promote intracellular delivery of polynucleic acids. *Gene Therapy, 8*(15), 1188-1196.

He, B., Kemppainen, J. A., Voegel, J. J., Gronemeyer, H., & Wilson, E. M. (1999). Activation function 2 in the human androgen receptor ligand binding domain mediates interdomain communication with the NH(2)-terminal domain. *Journal of Biological Chemistry, 274*(52), 37219-37225.

Hefner, E., Clark, K., Whitman, C., Behlke, M. A., Rose, S. D., Peek, A. S., & Rubio, T. (2008). Increased potency and longevity of gene silencing using validated Dicer substrates. *Journal of Biomolecular Techniques : JBT, 19*(4), 231-237.

Heyes, J., Palmer, L., Bremner, K., & MacLachlan, I. (2005). Cationic lipid saturation influences intracellular delivery of encapsulated nucleic acids. *J Control Release, 107*(2), 276-287.

Hirota, S., de Ilarduya, C. T., Barron, L. G., & Szoka, F. C., Jr. (1999). Simple mixing device to reproducibly prepare cationic lipid-DNA complexes (lipoplexes). *Biotechniques, 27*(2), 286-290.

Hornberg, E., Ylitalo, E. B., Crnalic, S., Antti, H., Stattin, P., Widmark, A., Bergh, A., & Wikstrom, P. (2011). Expression of androgen receptor splice variants in prostate cancer bone metastases is associated with castration-resistance and short survival. *PLoS One, 6*(4), e19059.

Horoszewicz, J. S., Leong, S. S., Kawinski, E., Karr, J. P., Rosenthal, H., Chu, T. M., Mirand, E. A., & Murphy, G. P. (1983). LNCaP Model of Human Prostatic Carcinoma. *Cancer Research, 43*(4), 1809-1818.

Hu, R., Lu, C., Mostaghel, E. A., Yegnasubramanian, S., Gurel, M., Tannahill, C., Edwards, J., Isaacs, W. B., Nelson, P. S., Bluemn, E., et al. (2012). Distinct transcriptional programs mediated by the ligand-dependent full-length androgen receptor and its splice variants in castration-resistant prostate cancer. *Cancer Research, 72*(14), 3457-3462.

Huang, Y. (2017). Preclinical and Clinical Advances of GalNAc-Decorated Nucleic Acid Therapeutics. *Molecular Therapy. Nucleic Acids, 6*, 116-132.

Huggins, C., & Hodges, C. V. (1941). Studies on Prostatic Cancer. I. The Effect of Castration, of Estrogen and of Androgen Injection on Serum Phosphatases in Metastatic Carcinoma of the Prostate. *Cancer Research, 1*(4), 293.

Jackson, A. L., & Linsley, P. S. (2010). Recognizing and avoiding siRNA off-target effects for target identification and therapeutic application. *Nature Reviews Drug Discovery, 9*, 57.

Jain, R. K., & Stylianopoulos, T. (2010). Delivering nanomedicine to solid tumors. *Nature Reviews Clinical Oncology, 7*(11), 653-664.

Janas, M. M., Schlegel, M. K., Harbison, C. E., Yilmaz, V. O., Jiang, Y., Parmar, R., Zlatev, I., Castoreno, A., Xu, H., Shulga-Morskaya, S., et al. (2018). Selection of GalNAc-conjugated siRNAs with limited off-target-driven rat hepatotoxicity. *Nature Communications, 9*(1), 723.

Jayaraman, M., Ansell, S. M., Mui, B. L., Tam, Y. K., Chen, J., Du, X., Butler, D., Eltepu, L., Matsuda, S., Narayanannair, J. K., et al. (2012). Maximizing the potency of siRNA lipid nanoparticles for hepatic gene silencing in vivo. *Angewandte Chemie International Edition, 51*(34), 8529-8533.

Jeffs, L. B., Palmer, L. R., Ambegia, E. G., Giesbrecht, C., Ewanick, S., & MacLachlan, I. (2005). A scalable, extrusion-free method for efficient liposomal encapsulation of plasmid DNA. *Pharmaceutical Research, 22*(3), 362-372.

Judge, A. D., Bola, G., Lee, A. C. H., & MacLachlan, I. (2006). Design of Noninflammatory Synthetic siRNA Mediating Potent Gene Silencing in Vivo. *Molecular Therapy, 13*(3), 494-505.

Juliano, R. L., & Stamp, D. (1978). Pharmacokinetics of liposome-encapsulated anti-tumor drugs: Studies with vinblastine, actinomycin D, cytosine arabinoside, and daunomycin. *Biochemical Pharmacology, 27*(1), 21-27.

Kantoff, P. W., Higano, C. S., Shore, N. D., Berger, E. R., Small, E. J., Penson, D. F., Redfern, C. H., Ferrari, A. C., Dreicer, R., Sims, R. B., et al. (2010). Sipuleucel-T immunotherapy for castration-resistant prostate cancer. *New England Journal of Medicine, 363*(5), 411-422.

Kawamura, E., Fielding, A. B., Kannan, N., Balgi, A., Eaves, C. J., Roberge, M., & Dedhar, S. (2013). Identification of novel small molecule inhibitors of centrosome clustering in cancer cells. *Oncotarget, 4*(10), 1763-1776.

Kim, D.-H., Behlke, M. A., Rose, S. D., Chang, M.-S., Choi, S., & Rossi, J. J. (2004). Synthetic dsRNA Dicer substrates enhance RNAi potency and efficacy. *Nature Biotechnology, 23*, 222.

Kimelberg, H. K., Tracy, T. F., Jr., Biddlecome, S. M., & Bourke, R. S. (1976). The effect of entrapment in liposomes on the in vivo distribution of [3H]methotrexate in a primate. *Cancer Research, 36*(8), 2949-2957.

Kulkarni, J. A., Darjuan, M. M., Mercer, J. E., Chen, S., van der Meel, R., Thewalt, J. L., Tam, Y. Y. C., & Cullis, P. R. (2018). On the Formation and Morphology of Lipid Nanoparticles Containing Ionizable Cationic Lipids and siRNA. *ACS Nano, 12*(5), 4787-4795.

Kulkarni, J. A., Tam, Y. Y. C., Chen, S., Tam, Y. K., Zaifman, J., Cullis, P. R., & Biswas, S. (2017). Rapid synthesis of lipid nanoparticles containing hydrophobic inorganic nanoparticles. *Nanoscale, 9*(36), 13600-13609.

Labrie, F., Dupont, A., Belanger, A., Lacoursiere, Y., Raynaud, J. P., Husson, J. M., Gareau, J., Fazekas, A. T., Sandow, J., Monfette, G., et al. (1983). New approach in the treatment of prostate cancer: complete instead of partial withdrawal of androgens. *Prostate, 4*(6), 579-594.

Lawrentschuk, N., & Klotz, L. (2011). Active surveillance for low-risk prostate cancer: an update. *Nature Reviews Urology, 8*(6), 312-320.

Lee, J. B., Zhang, K., Tam, Y. Y., Quick, J., Tam, Y. K., Lin, P. J., Chen, S., Liu, Y., Nair, J. K., Zlatev, I., et al. (2016). A Glu-urea-Lys Ligand-conjugated Lipid Nanoparticle/siRNA System Inhibits Androgen Receptor Expression In Vivo. *Molecular Therapy Nucleic Acids, 5*, e348.

Lee, J. B., Zhang, K., Tam, Y. Y., Tam, Y. K., Belliveau, N. M., Sung, V. Y., Lin, P. J., LeBlanc, E., Ciufolini, M. A., Rennie, P. S., et al. (2012). Lipid nanoparticle siRNA systems for silencing the androgen receptor in human prostate cancer in vivo. *International Journal of Cancer, 131*(5), E781-790.

Leung, A. K., Hafez, I. M., Baoukina, S., Belliveau, N. M., Zhigaltsev, I. V., Afshinmanesh, E., Tieleman, D. P., Hansen, C. L., Hope, M. J., & Cullis, P. R. (2012). Lipid Nanoparticles Containing siRNA Synthesized by Microfluidic Mixing Exhibit an Electron-Dense Nanostructured Core. *Journal of Physical Chemistry C: Nanomaterials and Interfaces, 116*(34), 18440-18450.

Li, Y., Alsagabi, M., Fan, D., Bova, G. S., Tewfik, A. H., & Dehm, S. M. (2011). Intragenic Rearrangement and Altered RNA Splicing of the Androgen Receptor in a Cell-Based Model of Prostate Cancer Progression. *Cancer Research, 71*(6), 2108.

Litwin, M. S., & Tan, H. J. (2017). The Diagnosis and Treatment of Prostate Cancer: A Review. *JAMA, 317*(24), 2532-2542.

Liu, C., Armstrong, C., Zhu, Y., Lou, W., & Gao, A. C. (2016). Niclosamide enhances abiraterone treatment via inhibition of androgen receptor variants in castration resistant prostate cancer. *Oncotarget, 7*(22), 32210-32220.

Liu, C., Lou, W., Zhu, Y., Nadiminty, N., Schwartz, C. T., Evans, C. P., & Gao, A. C. (2014). Niclosamide Inhibits Androgen Receptor Variants Expression and Overcomes Enzalutamide Resistance in Castration-Resistant Prostate Cancer. *Clinical Cancer Research, 20*(12), 3198.

Liu, L., & Dong, X. (2014). Complex impacts of PI3K/AKT inhibitors to androgen receptor gene expression in prostate cancer cells. *PLoS One, 9*(10), e108780.

Lonergan, P. E., & Tindall, D. J. (2011). Androgen receptor signaling in prostate cancer development and progression. *Journal of Carcinogenesis, 10*, 20.

Lv, H., Zhang, S., Wang, B., Cui, S., & Yan, J. (2006). Toxicity of cationic lipids and cationic polymers in gene delivery. *Journal of Controlled Release, 114*(1), 100-109.

Maeda, H. (2001). The enhanced permeability and retention (EPR) effect in tumor vasculature: the key role of tumor-selective macromolecular drug targeting. *Advances in Enzyme Regulation, 41*, 189-207.

Martin, S. K., Banuelos, C. A., Sadar, M. D., & Kyprianou, N. (2014). N-terminal targeting of androgen receptor variant enhances response of castration resistant prostate cancer to taxane chemotherapy. *Molecular Oncology, 9*(3), 628–639.

Maurer, N., Wong, K. F., Stark, H., Louie, L., McIntosh, D., Wong, T., Scherrer, P., Semple, S. C., & Cullis, P. R. (2001). Spontaneous entrapment of polynucleotides upon electrostatic interaction with ethanol-destabilized cationic liposomes. *Biophysical Journal, 80*(5), 2310-2326.

Mayer, L. D., Bally, M. B., & Cullis, P. R. (1986a). Uptake of adriamycin into large unilamellar vesicles in response to a pH gradient. *Biochimica et Biophysica Acta, 857*(1), 123-126.

Mayer, L. D., Hope, M. J., & Cullis, P. R. (1986b). Vesicles of variable sizes produced by a rapid extrusion procedure. *Biochimica et Biophysica Acta, 858*(1), 161-168.

McCaffrey, A. P., Meuse, L., Pham, T. T., Conklin, D. S., Hannon, G. J., & Kay, M. A. (2002). RNA interference in adult mice. *Nature, 418*(6893), 38-39.

McEwan, I. J. (2012). Intrinsic disorder in the androgen receptor: identification, characterisation and drugability. *Molecular Biosystems, 8*(1), 82-90.

Mottet, N., Bellmunt, J., Bolla, M., Briers, E., Cumberbatch, M. G., De Santis, M., Fossati, N., Gross, T., Henry, A. M., Joniau, S., et al. (2017). EAU-ESTRO-SIOG Guidelines on Prostate Cancer. Part 1: Screening, Diagnosis, and Local Treatment with Curative Intent. *European Urology, 71*(4), 618-629.

Mui, B. L., Tam, Y. K., Jayaraman, M., Ansell, S. M., Du, X., Tam, Y. Y. C., Lin, P. J. C., Chen, S., Narayanannair, J. K., Rajeev, K. G., et al. (2013). Influence of Polyethylene Glycol Lipid Desorption Rates on Pharmacokinetics and Pharmacodynamics of siRNA Lipid Nanoparticles. *Molecular Therapy. Nucleic Acids, 2*(12), e139.

Myung, J.-K., Banuelos, C. A., Fernandez, J. G., Mawji, N. R., Wang, J., Tien, A. H., Yang, Y. C., Tavakoli, I., Haile, S., Watt, K., et al. (2013). An androgen receptor N-terminal domain antagonist for treating prostate cancer. *The Journal of Clinical Investigation, 123*(7), 2948-2960.

Nakabayashi, M., Regan, M. M., Lifsey, D., Kantoff, P. W., Taplin, M. E., Sartor, O., & Oh, W. K. (2005). Efficacy of nilutamide as secondary hormonal therapy in androgen-independent prostate cancer. *BJU International, 96*(6), 783-786.

Nichols, J. W., & Deamer, D. W. (1976). Catecholamine uptake and concentration by liposomes maintaining pH gradients. *Biochimica et Biophysica Acta (BBA) - Biomembranes, 455*(1), 269-271.

Omidi, Y., Hollins, A. J., Benboubetra, M., Drayton, R., Benter, I. F., & Akhtar, S. (2003). Toxicogenomics of Non-viral Vectors for Gene Therapy: A Microarray Study of Lipofectin- and Oligofectamine-induced Gene Expression Changes in Human Epithelial Cells. *Journal of Drug Targeting, 11*(6), 311-323.

Omidi, Y., Hollins, A. J., Drayton, R. M., & Akhtar, S. (2005). Polypropylenimine dendrimer-induced gene expression changes: The effect of complexation with DNA, dendrimer generation and cell type. *Journal of Drug Targeting, 13*(7), 431-443.

Pan, C., Lara, P., Evans, C. P., Parikh, M., Dall'era, M., Liu, C., Robles, D., & Gao, A. (2018). Niclosamide in combination with abiraterone and prednisone in men with castration-resistant prostate cancer (CRPC): initial results from a phase Ib/II trial. *Journal of Clinical Oncology, 36*, 192-192.

Pearson, T., Shultz, L. D., Miller, D., King, M., Laning, J., Fodor, W., Cuthbert, A., Burzenski, L., Gott, B., Lyons, B., et al. (2008). Non-obese diabetic-recombination activating gene-1 (NOD-Rag1 null) interleukin (IL)-2 receptor common gamma chain (IL2r gamma null) null mice: a radioresistant model for human lymphohaematopoietic engraftment. *Clinical and Experimental Immunology, 154*(2), 270-284.

Pecot, C. V., Calin, G. A., Coleman, R. L., Lopez-Berestein, G., & Sood, A. K. (2011). RNA interference in the clinic: challenges and future directions. *Nature Reviews Cancer, 11*(1), 59-67.

Robbins, M., Judge, A. D., & MacLachlan, I. (2009). siRNA and innate immunity. *Oligonucleotides, 19*(2), 89-102.

Robinson, D., Van Allen, Eliezer M., Wu, Y.-M., Schultz, N., Lonigro, Robert J., Mosquera, J.-M., Montgomery, B., Taplin, M.-E., Pritchard, Colin C., Attard, G., et al. (2015). Integrative Clinical Genomics of Advanced Prostate Cancer. *Cell, 161*(5), 1215-1228.

Rose, S. D., Kim, D. H., Amarzguioui, M., Heidel, J. D., Collingwood, M. A., Davis, M. E., Rossi, J. J., & Behlke, M. A. (2005). Functional polarity is introduced by Dicer processing of short substrate RNAs. *Nucleic Acids Research, 33*(13), 4140-4156.

Sadar, M. D. (2011). Small molecule inhibitors targeting the "achilles' heel" of androgen receptor activity. *Cancer Research, 71*(4), 1208-1213.

Sahay, G., Querbes, W., Alabi, C., Eltoukhy, A., Sarkar, S., Zurenko, C., Karagiannis, E., Love, K., Chen, D., Zoncu, R., et al. (2013). Efficiency of siRNA delivery by lipid nanoparticles is limited by endocytic recycling. *Nature Biotechnology, 31*, 653.

Sathianathen, N. J., Konety, B. R., Crook, J., Saad, F., & Lawrentschuk, N. (2018). Landmarks in prostate cancer. *Nature Reviews Urology, 15*(10), 627-642.

Scher, H. I., Fizazi, K., Saad, F., Taplin, M. E., Sternberg, C. N., Miller, K., de Wit, R., Mulders, P., Chi, K. N., Shore, N. D., et al. (2012). Increased survival with enzalutamide in prostate cancer after chemotherapy. *New England Journal of Medicine, 367*(13), 1187-1197.

Semple, S. C., Akinc, A., Chen, J., Sandhu, A. P., Mui, B. L., Cho, C. K., Sah, D. W., Stebbing, D., Crosley, E. J., Yaworski, E., et al. (2010). Rational design of cationic lipids for siRNA delivery. *Nature Biotechnology, 28*(2), 172-176.

Semple, S. C., Klimuk, S. K., Harasym, T. O., Dos Santos, N., Ansell, S. M., Wong, K. F., Maurer, N., Stark, H., Cullis, P. R., Hope, M. J., et al. (2001). Efficient encapsulation of antisense oligonucleotides in lipid vesicles using ionizable aminolipids: formation of novel small multilamellar vesicle structures. *Biochimica et Biophysica Acta, 1510*(1-2), 152-166.

Sharp, A., Coleman, I., Yuan, W., Sprenger, C., Dolling, D., Rodrigues, D. N., Russo, J. W., Figueiredo, I., Bertan, C., Seed, G., et al. (2019). Androgen receptor splice variant-7 expression emerges with castration resistance in prostate cancer. *The Journal of Clinical Investigation, 129*(1), 192-208.

Sharp, A., Welti, J., Blagg, J., & de Bono, J. S. (2016). Targeting Androgen Receptor Aberrations in Castration-Resistant Prostate Cancer. *Clinical Cancer Research, 22*(17), 4280-4282.

Siegel, R. L., Miller, K. D., & Jemal, A. (2019). Cancer statistics, 2019. *CA: A Cancer Journal for Clinicians, 69*(1), 7-34.

Simpson, E. L., Davis, S., Thokala, P., Breeze, P. R., Bryden, P., & Wong, R. (2015). Sipuleucel-T for the Treatment of Metastatic Hormone-Relapsed Prostate Cancer: A NICE Single Technology Appraisal; An Evidence Review Group Perspective. *Pharmacoeconomics, 33*(11), 1187-1194.

Soloway, M. S., Schellhammer, P. F., Smith, J. A., Jr., Chodak, G. W., Vogelzang, N. J., & Kennealey, G. T. (1995). Bicalutamide in the treatment of advanced prostatic carcinoma: a phase II noncomparative multicenter trial evaluating safety, efficacy and long-term endocrine effects of monotherapy. *Journal of Urology, 154*(6), 2110-2114.

Sramkoski, R. M., Pretlow, T. G., Giaconia, J. M., Pretlow, T. P., Schwartz, S., Sy, M.-S., Marengo, S. R., Rhim, J. S., Zhang, D., & Jacobberger, J. W. (1999). A new human prostate carcinoma cell line, 22Rv1. *In Vitro Cellular & Developmental Biology - Animal, 35*(7), 403-409.

Suzuki, H., Sato, N., Watabe, Y., Masai, M., Seino, S., & Shimazaki, J. (1993). Androgen receptor gene mutations in human prostate cancer. *Journal of Steroid Biochemistry and Molecular Biology, 46*(6), 759-765.

Tam, Y. Y., Chen, S., Zaifman, J., Tam, Y. K., Lin, P. J., Ansell, S., Roberge, M., Ciufolini, M. A., & Cullis, P. R. (2012). Small molecule ligands for enhanced intracellular delivery of lipid nanoparticle formulations of siRNA. *Nanomedicine*, 665-674.

Tannock, I. F., de Wit, R., Berry, W. R., Horti, J., Pluzanska, A., Chi, K. N., Oudard, S., Théodore, C., James, N. D., Turesson, I., et al. (2004). Docetaxel plus Prednisone or Mitoxantrone plus Prednisone for Advanced Prostate Cancer. *New England Journal of Medicine, 351*(15), 1502-1512.

Tran, C., Ouk, S., Clegg, N. J., Chen, Y., Watson, P. A., Arora, V., Wongvipat, J., Smith-Jones, P. M., Yoo, D., Kwon, A., et al. (2009). Development of a second-generation antiandrogen for treatment of advanced prostate cancer. *Science, 324*(5928), 787-790.

Valencia-Sanchez, M. A., Liu, J., Hannon, G. J., & Parker, R. (2006). Control of translation and mRNA degradation by miRNAs and siRNAs. *Genes Dev, 20*(5), 515-524.

Van Etten, J. L., Nyquist, M., Li, Y., Yang, R., Ho, Y., Johnson, R., Ondigi, O., Voytas, D. F., Henzler, C., & Dehm, S. M. (2017). Targeting a Single Alternative Polyadenylation Site Coordinately Blocks Expression of Androgen Receptor mRNA Splice Variants in Prostate Cancer. *Cancer Research, 77*(19), 5228.

van Royen, M. E., van Cappellen, W. A., de Vos, C., Houtsmuller, A. B., & Trapman, J. (2012). Stepwise androgen receptor dimerization. *Journal of Cell Science, 125*(Pt 8), 1970-1979.

Veldscholte, J., Ris-Stalpers, C., Kuiper, G. G., Jenster, G., Berrevoets, C., Claassen, E., van Rooij, H. C., Trapman, J., Brinkmann, A. O., & Mulder, E. (1990). A mutation in the ligand binding domain of the androgen receptor of human LNCaP cells affects steroid binding characteristics and response to anti-androgens. *Biochemical and Biophysical Research Communications, 173*(2), 534-540.

Walsh, P. C., Lepor, H., & Eggleston, J. C. (1983). Radical prostatectomy with preservation of sexual function: anatomical and pathological considerations. *Prostate, 4*(5), 473-485.

Wang, H., Tam, Y. Y., Chen, S., Zaifman, J., van der Meel, R., Ciufolini, M. A., & Cullis, P. R. (2016). The Niemann-Pick C1 Inhibitor NP3.47 Enhances Gene Silencing Potency of Lipid Nanoparticles Containing siRNA. *Molecular Therapy, 24*(12), 2100-2108.

Ware, K. E., Garcia-Blanco, M. A., Armstrong, A. J., & Dehm, S. M. (2014). Biologic and clinical significance of androgen receptor variants in castration resistant prostate cancer. *Endocrine-Related Cancer, 21*(4), T87-103.

Wei, X. X., Fong, L., & Small, E. J. (2015). Prostate Cancer Immunotherapy with Sipuleucel-T: Current Standards and Future Directions. *Expert Review of Vaccines, 14*(12), 1529-1541.

Welti, J., Rodrigues, D. N., Sharp, A., Sun, S., Lorente, D., Riisnaes, R., Figueiredo, I., Zafeiriou, Z., Rescigno, P., de Bono, J. S., et al. (2016). Analytical Validation and Clinical Qualification of a New Immunohistochemical Assay for Androgen Receptor Splice Variant-7 Protein Expression in Metastatic Castration-resistant Prostate Cancer. *European Urology, 70*(4), 599-608.

Whitehead, K. A., Langer, R., & Anderson, D. G. (2009). Knocking down barriers: advances in siRNA delivery. *Nature Reviews Drug Discovery, 8*(2), 129-138.

Yamamoto, Y., Lin, P. J. C., Beraldi, E., Zhang, F., Kawai, Y., Leong, J., Katsumi, H., Fazli, L., Fraser, R., Cullis, P. R., et al. (2015a). siRNA Lipid Nanoparticle Potently Silences Clusterin and Delays Progression When Combined with Androgen Receptor Cotargeting in Enzalutamide-Resistant Prostate Cancer. *Clinical Cancer Research, 21*(21), 4845-4855.

Yamamoto, Y., Loriot, Y., Beraldi, E., Zhang, F., Wyatt, A. W., Nakouzi, N. A., Mo, F., Zhou, T., Kim, Y., Monia, B. P., et al. (2015b). Generation 2.5 Antisense Oligonucleotides Targeting the Androgen Receptor and Its Splice Variants Suppress Enzalutamide-Resistant Prostate Cancer Cell Growth. *Clinical Cancer Research, 21*(7), 1675.

Yang, Y. C., Banuelos, C. A., Mawji, N. R., Wang, J., Kato, M., Haile, S., McEwan, I. J., Plymate, S., & Sadar, M. D. (2016). Targeting Androgen Receptor Activation Function-1 with EPI to Overcome Resistance Mechanisms in Castration-Resistant Prostate Cancer. *Clinical Cancer Research, 22*(17), 4466.

Yoshimura, K., Sumiyoshi, Y., Hashimura, T., Ueda, T., Kamiryo, Y., Yamamoto, A., & Arai, Y. (2003). Neoadjuvant flutamide monotherapy for locally confined prostate cancer. *International Journal of Urology, 10*(4), 190-195.

Zhigaltsev, I. V., Belliveau, N., Hafez, I., Leung, A. K., Huft, J., Hansen, C., & Cullis, P. R. (2012). Bottom-up design and synthesis of limit size lipid nanoparticle systems with aqueous and triglyceride cores using millisecond microfluidic mixing. *Langmuir, 28*(7), 3633-3640.

Zimmermann, T. S., Lee, A. C. H., Akinc, A., Bramlage, B., Bumcrot, D., Fedoruk, M. N., Harborth, J., Heyes, J. A., Jeffs, L. B., John, M., et al. (2006). RNAi-mediated gene silencing in non-human primates. *Nature, 441*(7089), 111-114.

Appendices

Appendix A Mean relative tumor volumes and biological replicates of 22Rv1 xenografts (Chapter 3.6)

Tumor volumes (in mm^3) were assessed by external caliper measurements throughout the antitumor study. The following table compares the relative tumor volumes between the siARv-LNP, siARfl-LNP, siLUC-LNP, and PBS control treatment groups, and indicates the biological replicates for each measurement. Relative tumor volume represents tumor volume on indicated treatment day normalized to tumor volume on treatment day 0. Tumor volume measurements were not taken on day 20, end of study.

Group	Treatment day							
	3	5	7	10	12	14	17	19
siARv-LNP	1.395±0.077	1.901±0.153	2.241±0.182	2.857±0.287	3.872±0.384	5.347±0.526	7.541±0.809	9.150±1.377
	n=11	n=11	n=11	n=11	n=10	n=10	n=10	n=7
siARfl-LNP	1.323±0.070	1.895±0.114	2.542±0.202	2.856±0.347	5.754±0.547	7.930±0.905	11.855±1.465	14.233±2.302
	n=10	n=10	n=10	n=10	n=10	n=9	n=8	n=6
siLUC-LNP	1.457±0.071	1.925±0.110	2.515±0.161	3.785±0.333	5.492±0.420	7.327±0.696	10.194±1.020	12.566±1.525
	n=11	n=11	n=11	n=11	n=11	n=9	n=8	n=7
PBS	1.922±0.096	2.515±0.186	3.409±0.307	6.079±0.678	8.150±0.730	9.498±1.295	12.358±2.316	18.573±3.770
	n=11	n=11	n=11	n=11	n=9	n=6	n=5	n=4